NASA

Technical Memorandum 81991

Energetic Particles in the Pre-Dawn Magnetotail of Jupiter

A. W. Schardt, F. B. McDonald, and J. H. Trainor

AUGUST 1980

National Aeronautics and Space Administration

Goddard Space Flight Center
Greenbelt, Maryland 20771

ENERGETIC PARTICLES IN THE PRE-DAWN MAGNETOTAIL OF JUPITER

A.W. Schardt, F.B. McDonald and J.H. Trainor

Laboratory for High Energy Astrophysics
NASA/Goddard Space Flight Center
Greenbelt, Maryland 20771 USA

ABSTRACT

A detailed account is given of the energetic electron and proton populations as observed with Voyagers 1 and 2 during their passes through the dawn magnetotail of Jupiter. In general the results of the Pioneer 10 pass at 90° to the Jupiter-Sun line have been confirmed and extended. The region between 20 and 150 R_J is dominated by a thin plasma sheet, and open field lines were observed at 42 R_J at a magnetic latitude of only 15°. Trapped energetic electron and proton fluxes reach their maximum in the plasma sheet and decrease rapidly even a few degrees away from it. The spectra of trapped protons can be represented by an exponential in rigidity and have a characteristic energy of ~ 50 keV. Proton anisotropies in the plasma sheet were consistent with corotation even at 100 R_J, but the preliminary analysis is not yet conclusive. A major proton acceleration event as well as several cases of field-aligned proton streaming were observed. Comparable proton fluxes were observed in the plasma sheet by Voyagers 1 and 2. The flux of > 0.4 MeV protons decreases by three orders of magnitude between 20 and 90 R_J and then remains relatively constant to the boundary layer near the magnetopause. Between 20 and 30 R_J in the anti-solar direction, the trapping region has a latitudinal extent which is comparable to that observed during the inbound pass at -30° solar aspect. The plasma sheet positions in the magnetotail can be represented by a distorted disk which rotates about the Jovian spin axis. Fine structure in the data indicate longitudinal asymmetries with respect to the dipole orientation. Electron spectra in the outer magnetosphere, the magnetosheath and interplanetary space are modulated by the Jovian longitude relative to the subsolar point; this confirms the Pioneer 10 and 11 results.

Introduction

The Voyager 1 and 2 passes by Jupiter offered the first opportunity since 1974 to perform in situ investigations of the Jovian magnetosphere. The cosmic ray subsystem (CRS) observed energetic electrons and protons between 0.4 and 10 MeV and ions above 1.8 MeV/nucleon. The latter results are described in the companion paper. While the outbound trajectory passed through the dawn magnetotail, a previously unexplored region, the inbound trajectory through the subsolar hemisphere followed relatively closely the path previously taken by Pioneers 10 and 11 (Fig. 1). Summaries of the new results were published by Vogt et al. (1979a,b).

The two passes through the subsolar hemisphere confirmed in general the Pioneer results (a summary and references to the Pioneer results are given in the review article by Goertz and Thomsen, 1979). As expected, the magnetopause position was variable and several crossings were observed between 45 and 80 R_J (Jupiter radii). In the outer magnetosphere (>45 R_J) fluxes of low energy protons (0.4 to 3 MeV) were variable but showed no consistent 10-hour modulation. High-energy electrons (>8 MeV) did show a modulation which was in phase with prediction from the so-called clock model (Chenette et al., 1974; Smith et al., 1976).

Inside 40 R_J, a well-developed current sheet was encountered which was closely aligned with the magnetic equator. Because of the 10.4° tilt between the magnetic dipole and Jupiter's spin axis, this current sheet moved up and down with Jupiter's 10-hour period. Since Voyager was always within 5° of the equator, two crossings occurred every 10 hours. Fluxes of both energetic electrons and protons peaked at the magnetic equator. In the case of Voyager 1, the proton fluxes observed at the crossing near λ_{III} = 300° (1965) were 30 to 70% more intense than those associated with the crossing near λ_{III} = 100°. No such

consistent difference was present in the Voyager 2 data. The Voyager 1 observations suggest that an asymmetry exists at times in the flux of trapped energetic particles which may be associated with the so-called active and inactive hemispheres (Vasyliunas, 1975; Dessler, 1978).

In the inner magnetosphere, absorption features in the low-energy proton population (~2 MeV) were associated with Ganymede, Europa and Io. During its inbound pass, Voyager 2 came within 63,000 km of Ganymede; the large disturbances in the proton flux which correlate with similar disturbances in magnetic field and plasma parameters have been ascribed to a possible wake created by Ganymede's motion through the magnetospheric plasma (Burlaga et al., 1980). Near Ganymede's orbit, Simpson et al. (1975) had previously observed with Pioneer 11 numerous bursts of ~1 MeV protons which typically lasted less than 1 minute, but the magnetic field signature observed at the same time was quite different (Kivelson and Wing, 1976) from that observed by Voyager 2. As already noted from Pioneer data, the Io-associated decrease in proton flux starts at $L \approx 6.2$, well outside of Io's orbit and appears to be primarily due to interactions with the Io plasma torus rather than geometric absorption by Io itself.

The major new region investigated, and to be discussed in this paper, is the dawn magnetotail (Fig. 1, Table 1). The Pioneer 10 and Voyager outbound passes provide data between -100° and -135° from the Jupiter-Sun line all the way out to the magnetopause and in the anti-solar direction (Midnight) at 21 R_J. As in the case of Pioneer 10, we found a thin plasma sheet at the magnetic equator which was already well developed near 23 R_J. Sharp flux maxima in proton and electron (<3 MeV) population occurred near the sheet and permitted us to follow the position of the plasma sheet out to 160 R_J. At a latitude of $\sim 15^{\circ}$ away from the plasma sheet, the proton flux dropped to its interplanetary value.

The proton spectra observed in the magnetotail agreed generally with those

observed during the outbound pass of Pioneer 10; however, we have now spectra measured in different directions relative to the magnetic field. Most of the time, observed spectral differences are small and reflect the effects of corotation and of spatial gradients of the proton spectrum. At times, the plasma sheet was active and quite different spectra were observed parallel and perpendicular to the field. Proton streaming along the field and away from Jupiter was observed on several occasions with anisotropies as high as 400:1. In the plasma sheet at 155 R_J, Voyager 2 observed a very anisotropic (20:1) proton flow which was apparently accompanied by a super Alfvenic flow of an oxygen-sulfur plasma away from Jupiter (Krimigis, et al. 1980).

The many new observations of the plasma sheet position place additional constraints on the models developed after the Pioneer missions. Our data agree best with a model that involves a gradual bending of the plasma sheet towards the Jovigraphic equator (Bridge et. al., 1979). Since a much smaller or no bending was observed with Pioneer-10, we have to assume that conditions in the plasma sheet changed between 1973 and 1979. An alternate model keeps the plasma sheet inclination fixed at 10.4^{o} and accounts for the differences on the basis of different longitudes at which the plasma sheet was crossed. The latter model, however, does not explain the absence of plasma sheet crossings beyond 80 R_J during the Voyager 1 mission.

The periodic modulation of the energetic electron flux continues in the magnetosheath and interplanetary space (Chenette et al., 1974); however, the character of this modulation is different from that observed in the plasma sheet region. The proton flux does not participate in this modulation, and minima in the energetic electron flux occur simultaneously at all places where it has been observed, hence the name "clock" modulation. This modulation must be caused by an asymmetry that rotates with Jupiter (Dessler and Hill, 1975), and we show that it is apparently directly associated with the active hemisphere.

Instrumentation

As its name implies, the CRS was designed for cosmic ray studies (Stone et al., 1977). It consists of two High Energy Telescopes (HET), four Low Energy Telescopes (LET) and The Electron Telescope (TET). The detectors have large geometric factors (~0.48 to 8 cm^2 ster) and long electronic time constants (~24 μsec) for low power consumption and good stability. Normally the data are primarily derived from comprehensive (ΔE_1, ΔE_2 and E) pulse-height information about individual events. Because of the high particle fluxes encountered at Jupiter, greater reliance had to be placed on counting rates in single detectors and various coincidence rates. The detectors used for most of our work are listed in Table 2. In interplanetary space, guard counters are placed in anti-coincidence with the primary detectors to reduce the background from high-energy particles penetrating through the sides of the telescopes. These guard counters were turned off in the Jovian magnetosphere, when the accidental anti-coincidence rate became high enough to block a substantial fraction of the desired counts. Fortunately, under these conditions the spectra were sufficiently soft that the background due to penetrating particles was small.

The data on proton and ion fluxes at Jupiter were obtained with the Low Energy Telescope, LET (Fig. 2 and Table 2). The thicknesses of individual solid-state detectors in the LET and their trigger thresholds were chosen such that even in the Jovian magnetosphere, electrons made no contribution to the proton counting rates (Lupton and Stone, 1972). Dead time corrections and accidental coincidences were small (<20%) throughout most of the magnetotail but were substantial (>50%) at flux maxima within 40 R_J of Jupiter. Results in this paper are based only on data obtained on the rising part of the detector response (prior to roll over) and were corrected with the dead time appropriate to the detector (22 to 25 μsec). The high counting rates, however, caused some baseline shift which was insignificant compared to the energy of heavy ions (Carbon to

Sulfur) but may have raised proton thresholds significantly. In the inner magnetosphere, the L_2 counting rate was still useful because it never rolled over. This rate is due to 1.8 to 13 MeV protons penetrating L_1 (0.43 cm^2 ster) and >9 MeV protons penetrating the shield (8.4 cm^2 ster). For an E^{-2} spectrum, the two groups would make comparable contributions; but in the magnetosphere for the E^{-3} to E^{-4} spectrum above 2.5 MeV (McDonald et al., 1979), the contribution from protons penetrating the shield would be only 3 to 14%.

The LET $L_1L_2\overline{L_4}$ coincidence-anticoincidence rate gives an accurately defined proton flux between 1.8 and 8 MeV with a very small alpha particle contribution ($\sim 10^{-3}$). Corrections are required for dead time losses in L_1, accidental L_1L_2 coincidences, and anticoincidence losses from L_4. The anticcincidence time constant was count-rate dependent; for low rates it was 27 μsec and gradually decreased to 10 μsec at maximum counting rate. A third-order polynomial in the L_4 rate was used to express the anticoincidence dead time. In correcting for accidental coincidences between L_1 and L_2, account was taken of the fact that a major fraction of the counts in L_2 were in coincidence with L_1. An average accidental coincidence time constant of 16 μsec was used. The actual accidental coincidence time constant was in the range of 10 to 25 μsec with a complex dependence on pulse height and rate.

In addition to the rates listed in Table 2, the energy lost in detectors L_1, L_2 and L_3 was measured for individual particles. For protons this covered the energy range from 0.42 to 8.3 MeV. Protons can be identified positively by the ΔE vs. E technique, their spectra obtained and accidental coincidences greatly reduced. Because of telemetry limitations, however, only a small fraction of the events could be transmitted, and statistics become poor unless pulse-height data are averaged over one hour for one detector or 15 minutes when summed over the four LETs.

Each Voyager spacecraft carried four LETs; three of these looked in mutually-perpendicular directions such that LET-A, -D and -B formed a right-handed coordinate system. LET-C looked in the minus A direction. Figure 3 shows the typical directions in which the telescopes were pointed during the outbound passes of Voyager 1. The actual directions beyond 30 R_J were within ±15° of those shown in Figure 3, which gives the exact directions for Voyager 1 at 50 R_J. LET-B was nearly parallel to the average magnetic field during the outbound pass, and the other three telescopes looked almost perpendicular to the field. LET-A pointed 66° north from the plane of the ecliptic but otherwise towards the corotation direction, and LET-D pointed nearly in the corotation direction. Relative intensities and differences in energy spectra for these directions can be determined. If higher-order anisotropies are small compared to the first-order anisotropy, then the average flux, first-order anisotropy and its direction can be determined uniquely. At Jupiter, however, the first- and second-order anisotropies are often comparable (McDonald et al., 1979), and such a simple analysis would be misleading except when two or three detectors point perpendicular to the magnetic field.

One HET and two LETs share the same data lines and pulse-height analyzers; thus the three telescopes can interfere with one another during periods of high counting rates. To avoid this and explore different coincidence conditions, the experiment was cycled through four operating modes, each 192 seconds long. Either the HET or the two LETs were turned on at a time. The LETs were cycled through L_1 only, and L_1L_2 coincidence requirements. Some of the time, one of the LETs was operated only in the $L_1L_2L_3$ coincidence mode to improve statistics for higher energy particles and reduce interference from spacecraft noise. Inside of 20 R_J, both HETs and two LETs were turned off, and the remaining two LETs were operated in the double coincidence mode on Voyager 1 and triple mode on Voyager 2. The TET was

cycled through various conicidence conditions, including singles from the front detectors. At the expense of some time resolution, this procedure permitted us to obtain significant data in the middle magnetosphere and excellent data during the long passage through the magnetotail region.

Particle Fluxes in the Magnetotail

An overview of the energetic particle fluxes encountered during the outbound passes of Voyagers 1 and 2 is shown in figures 4 and 5. These spacecraft and Pioneer 10 went towards the dawn direction between -100° and -135° from the Jupiter-Sun direction. The deep modulation observed in the particle fluxes (Voyager 1) indicates that the plasma sheet is much thinner between 20 and 40 R_J than in the subsolar direction. Periodic plasma sheet crossings or approaches can be identified beyond 150 R_J. In contrast, no clear cut modulation of low energy proton fluxes has been seen beyond 45 R_J in the subsolar hemisphere.

The latitudinal extent of the energetic particle trapping region is probably controlled by a pressure balance between the Jovian magnetic field, trapped thermal plasma, and solar wind pressure. The interactions between forces due to the Jovian magnetic field and centrifugal forces concentrate the plasma into a sheet near the equator (Gleeson and Axford, 1976). In the subsolar hemisphere, the addition of the solar wind pressure insures that the sheet is relatively thick. When a section of the magnetosphere rotates from the subsolar hemisphere into the antisolar direction, the trapped thermal plasma can expand radially outward because the solar wind pressure is removed. The expansion speed is limited by the wave velocity to be discussed later (Table 5). This velocity limits the expansion during the 4 to 5 hours available for crossing the tail. The thinnest trapping region should therefore occur just before the expansion is

stopped, when the expanding region rotates into the dawn magnetopause. Comparison between Voyager 1 and 2 data from 20 to 40 R_J shows that the trapping region is thicker in the antisolar direction (Voyager 2) than in the dawn direction. The difference in modulation between the two missions is partially due to different latitudes at equal distances from Jupiter; however, some direct comparisons are possible. The peak fluxes at equatorial crossings are comparable and decrease with distance. In contrast, Voyager 1 measured a smaller flux of 0.42 to 12 MeV protons at 24.4 R_J and only 7° below the magnetic equator (281/cm^2 sec ster) than Voyager 2 at 34.5 and 40.3 R_J at 10° and 9.2° below the equator (648 and 458/cm^2 sec ster, respectively).

The valleys in the modulation of the proton flux approach interplanetary values beyond 40 to 60 R_J. The interplanetary proton flux was due to corotating solar streams, and Conlon et al. (1979) has shown that the flux observed in the tail away from the plasma sheet was within a factor of 2 of intensities observed by the sister spacecraft at a time corresponding to the solar corotation delay. This effect accounts for reduction of the 10-hour modulation of the Voyager 2 proton flux (> 1.8 MeV) between 105 and 130 R_J (Fig. 4). The electron flux was not affected by the proton enhancement and was modulated by the position of the plasma sheet relative to the spacecraft.

On the average the maxima of both electron and proton fluxes decrease monotonically from 20 to 90 R_J and remain relatively constant from there to the boundary layer near the magnetopause. From the character of the electron flux (figure 5) it appears that Voyager 2 was either in the boundary layer or sheath from 170 R_J until its final magnetosphere crossing. All three spacecraft (Pioneer 10, Voyager 1 and 2) encountered enhanced particle fluxes at their first magnetopause crossings; however, such enhancements in the proton flux were not necessarily associated with later crossings (Fig. 5). These enhancements were

probably due to local acceleration when the magnetopause was being compressed prior to its first passage over the spacecraft.

Proton Spectra

The differential proton spectra observed during the Voyager and Pioneer 10 outbound passes can be approximated either by a power law in energy, $j(E) = K E^{-\gamma}$ or somewhat better by an exponential in rigidity $j(p) = ke^{-p/p_o}$, where p_o is the e-folding momentum (McDonald et al., 1979). Figure 6 shows typical Voyager 1 spectra observed at flux maxima at distances of 34.2, 64.9, 116.9, and 146 R_J. The spectra can be characterized by the energy corresponding to the e-folding momentum, $E_o = (p_o/43.32)^2$, which falls into the range of 30 to 80 keV. In contrast the spectra at flux minima are much harder, $0.5 \leq E_o \leq 2$ MeV, and are characteristic of corotating events (Van Hollebeke et al. 1978). The first such spectrum was seen at ~42.4 R_J and is shown in figure 6.

Figure 7 shows the spectral index E_o and 1 MeV flux derived from least squares fit to 1 hour average pulse-height data from LET A of Voyager 1. The regular pattern of soft spectra at flux maxima (plasma sheet crossings) is followed with few exceptions. These results are complemented by data from the outbound pass of Pioneer 10 (Fig. 8),which provides a better spatial resolution for the behavior of the spectral index in the plasma sheet. Since Pioneer 10 was at a latitude of ~9°, the plasma sheet approached and receded from it more gradually; additionally, the spectrum could be determined every 15 minutes. The Pioneer 10 observations show that the spectrum of trapped particles is hardest at the center of the plasma sheet and becomes significantly softer a short distance (~1°) above it. The new results show

that even further away the spectrum of energetic protons becomes harder because of the presence of interplanetary particles which are not trapped.

Normally, only small differences existed between spectra observed in different directions (LET A, B, and D). Most of the time the spectrum in LET D was somewhat harder than in A. Two effects contribute to this hardening. One of these is the change in spectrum due to the Compton-Getting effect. Let ϕ be the angle between the anti-corotation direction and the direction in which the detector points, thus the Compton-Getting effect makes its largest contribution at $\phi=0$. If the energy spectrum in the (partially) corotating frame can be approximated by $j(E_c)=K\,E_c^{-\gamma}$ near the energy E_c, then to first order in ε, the spectral index γ' looking into ($\phi=0$) and along ($\phi=180$) the corotation direction are given by (Ipavich, 1974):

$$\gamma' = \gamma + (\gamma+1)\,\varepsilon \qquad \phi = 0$$
$$\gamma' = \gamma - (\gamma+1)\,\varepsilon \qquad \phi = 180^{\circ} \qquad (1)$$

where $\varepsilon = \sqrt{E_{cr}/E}$ and E_{cr} is the particle's (partial) corotation energy. However, velocities corresponding to E_{cr} in the 500 to 1500 km/sec range at 35 to 65 R_J would be required if this were the only effect. The rigid corotation velocities are 440 and 816-km/sec, respectively, at 35 and 65 R_J. The second and apparently equally important cause is the change in spectral parameter E_o (Fig. 7) away from the plasma sheet. Above or below the center of the plasma sheet, the direction of the magnetic field is nearly radially away from Jupiter; thus, positive ions with a guiding center one gyroradius (ρ_g) closer to the center of the plasma sheet will be counted as moving in the corotation direction. As a result LET A, which points 69° from the anticorotation direction, sees protons whose guiding center is 0.4 ρ_g closer to the center of the plasma sheet; $\rho_g \approx 0.3$ R_J for 2 MeV protons at 45 R_J in the tail.

Similarly, LET D sees protons attached to field lines ~1 ρ_g further away from the center. As a result LET D detects a larger admixture of solar cosmic rays than LET A.

During the outbound pass of Voyager 1, the LET B telescope pointed towards the planet often almost antiparallel to a field line (Fig. 3), particularly when Voyager was just above the center of the plasma sheet. Consequently, LET A, C, and D pointed nearly perpendicular to the magnetic field and could measure the anisotropy of particles with 90° pitch angles. This permits a determination of the non-gyrotropic component perpendicular to $\bar{B}$, without requiring knowledge of the pitch angle distribution. Only the Compton-Getting and flux gradient effects contribute to the anisotropy in that plane (Birmingham and Northrop, 1979). Using again a local power law approximation, we can express the ratio in counts between two detectors as follows (to first order in ε):

$$\frac{j(E,\phi_1)}{j(E,\phi_2)} = \frac{1 + \rho_g \left|\frac{\partial \ln j}{\partial z}\right| \cos\theta_1}{1 + \rho_g \left|\frac{\partial \ln j}{\partial z}\right| \cos\theta_2} \left(\frac{1 - 2\,\varepsilon \cos\phi_2}{1 - 2\,\varepsilon \cos\phi_1}\right)^{\gamma+1} \qquad (2)$$

where ϕ is the detector look angle relative to the corotation direction, with ϕ=0 when the detector looks into the corotation direction. θ is the angle between the detector pointing direction and the direction ($\nabla j \times \bar{B}$) in which the intensity gradient makes the largest contribution to the flux. In the tail geometry, θ is approximately equal to ϕ because the flux gradient is approximately north-south in the Z-direction. The differential flux $j(E,\phi)$ is the flux perpendicular to $\bar{B}$ that is the flux of 90° pitch angle particles. The gradient term constitutes a major uncertainty in this expression. This

term was estimated using the flux increase towards maximum and distance to the center of the plasma sheet based on the bent twisted disk model (see Section Plasma Sheet Crossings). However, local gradients may be different from average gradients, and even the average gradient is uncertain because the motion of the neutral sheet may deviate from the model.

Preliminary calculations were performed with 2 MeV protons for the rise towards the flux maxima at 34 and 103 R_J and near the flux minima at 50 and 107 R_J (Fig. 7). These positions were chosen because of the close alignment between the magnetic field (Ness, private communication) and LET B. The results shown in Table 3 are generally consistent with corotation. A significantly larger anisotropy is observed near flux maxima because of the softer spectrum and contribution from the flux gradient, the gradient being either zero or very small near flux minima. It should be emphasized, however, that these preliminary results are inadequate to firmly establish corotation or a lack there of. The ratios between counts in different detectors varies a great deal, but it is expected that a more systematic analysis of these anisotropies will contribute towards resolving this question.

The plasma sheet crossing at 59 R_J was unusual in that the spectrum became harder rather than softer near the plasma sheet (Fig. 7) and spectra observed with LET A, B, and D were different from one another (Fig. 6). The magnetic field data indicate that the region in which the field reverses is crossed rapidly compared to the ~ 1 hr. 4 min. over which our data had to be averaged; therefore, most of the time the spacecraft was either just above or below the center of the plasma sheet, and the magnetic field was aligned with LET B (except at the instant of crossing). At 2 MeV the LET A/LET D ratio is 4.0 corresponding to a first order anisotropy of 0.70; the Compton-Getting effect can account for at most 0.30 of this. A local flux increase of 2.6 times per R_J towards the center of the plasma sheet is required to explain the observed

anisotropy (ρ_g = 0.4 R_J in the 7 gamma field).Typically, a factor of 1.5 was observed at other times. Particles with 90° pitch angles, LET A and D, have a much harder spectrum than the small pitch angle particles seen by LET B. This is exactly what would be seen if the acceleration occurred locally in the low field region of the plasma sheet, and a substantial fraction of the particles mirror in the 7 gamma field near the spacecraft. A considerably less extreme example of local acceleration was observed by Pioneer 10 at 45 R_J (Fig. 8). The usual plasma sheet value E_0 ≈ 50 keV increased at this crossing to 150 keV; however, this is a spin-averaged value and the spectra perpendicular to the magnetic field may well have been harder. The Voyager 2 magnetotail proton spectra appear to be in general agreement with the Voyager 1 data; however, no major acceleration event was found.

Proton Streaming

Most of the time the counting rate ratio between the different LET's fell into the range of 1 to 2 with the higher flux perpendicular to $\overline{B}$. Ratios in this range are consistent with expected pitch angle distributions (McDonald et al., 1979) and corotation and gradient anisotropies. Major departures from this condition were observed at a number of occasions between 98 and 200 R_J by both Voyager 1 and 2. These events are characterized by rapid flux changes and a large enhancement in the flux of protons coming from the general direction of Jupiter.

The first example of streaming was observed at 98 R_J with Voyager 1 on March 11, 1979, from 0500 to 0700 spacecraft time. On the basis of 15-minute average magnetic field values (Ness, private communication), LET B pointed during this period between 20° and 31° from the anti-field direction, and the

spacecraft was near but did not cross the center of the plasma sheet; LET A looked perpendicular to the field. Figure 9 shows a histogram of the counting rates of the >0.4 MeV proton flux taken every 192 seconds. Due to cycling of the detectors, LET A and B were turned off when HET I was on. In Figure 9, data gaps in the LET B histogram are bridged with a dotted line. This event is characterized by large (at least 400 times) increases in the field-aligned flux and moderate (10 times) or no increases in the flux perpendicular to $\vec{B}$. Each of these increases lasted about 10 minutes. The maximum field-aligned flux was about 40 times the flux normally found in the plasma sheet.

As Figure 10 shows, the spectra of the two proton populations are also quite different. The 97.9 R_J spectra in Figure 10 represent an average from 0448 to 0552 spacecraft time on 3/11/79, and the 98.6 R_J spectra were averaged from 0552 to 0656. As can be seen from Figure 9, these periods cover most of the intense activity. The spectrum and average intensity of streaming protons is characteristic of the trapped proton population in the plasma sheet (compare Figs. 6 and 10). The spectra and intensities of locally mirroring protons are characteristic of interplanetary protons. The relative fluxes and spectra indicate that we observed field-aligned streaming of energetic protons characteristic of the normally trapped plasma sheet population. Peak intensities in LET B were as high as those found at ~40 R_J. The most likely cause is a field line reconfiguration (magnetic merging?) between Jupiter and Voyager 1 which injected protons onto open field lines. This process was probably associated with proton acceleration because no corresponding changes were found in the electron population. If the electrons were closely collimated along the magnetic field, however, we could have missed streaming electrons because the detector geometry was less favorable.

Five proton streaming events are listed in Table 4. The second event

observed with Voyager 1 at 133 R_J resembled the earlier event. The event observed at 188 R_J in the magnetosheath was quite different in that we observed a much smaller anisotropy, and electron fluxes were also affected. Similar observations have been made in the terrestrial magnetosphere (Sarris et al., 1976 and references therein). Sarris found that proton and electron bursts are always associated in the magnetosheath. In the earth's magnetotail, they are generally but not always associated. The closest terrestrial analog to our magnetotail observations are probably impulsive proton bursts (Sarris et al., 1976) that are not accompanied by electron bursts; however, they lasted only a few seconds as compared to over 10 minutes in the case of the Jovian bursts.

The Voyager 2 observations of highly anisotropic fluxes (Table 4) differed from those of Voyager 1 in that the magnetic field direction was disturbed during the Voyager 2 observations. It is possible, therefore, that the large anisotropy was not field-aligned but had a major perpendicular component. This would require either unreasonably large flux gradients or high plasma convection velocities. Krimigis et al., (1980) have analyzed the proton and heavier ion spectra associated with the 155 R_J event and concluded the they were probably seeing an oxygen-sulfur plasma moving away from Jupiter with a velocity corresponding to a mean ion energy of 100 keV.

In summary, we have observed three different types of proton streaming events. Well inside the magnetopause at 98 and 133 R_J, we detected field-aligned streaming in the plasma sheet in an ordered magnetic field configuration. Near the magnetopause, but still inside the magnetosphere, the large anisotropies appear to be due to a combination of fast plasma motion coupled with field-aligned flow in an irregular field configuration, and in the dawn magnetosheath we see proton and electron streaming. These

observations have many similarities with analogous observations at earth as reported by Sarris et al., (1976) and by Frank et al., (1976) in his "fireball" observations.

Plasma Sheet Crossings

Models of the plasma sheet position in the dawn direction have been developed to account for the Pioneer 10 outbound data (see, for example, Smith et al., 1974; Goertz et al., 1976, Northrop et al., 1976; Kivelson et al., 1978). These models can now be tested against the Voyager 1 and 2 results. To simplify comparison with experimental results, plasma sheet positions are expressed in terms of R, δ, λ coordinates, that is radius, latitude from the Joviographic equator and longitude λ_{III} (1965). The simplest model places the plasma sheet at the dipole equator and λ as a function of δ is given by the equation of a plane tilted at an angle β to the rotational equator:

$$\lambda = \lambda_d \mp \cos^{-1} \frac{\tan \delta}{\tan \beta} \quad (3)$$

where λ_d is the longitude to which the dipole points in the southern hemisphere (20.8°), and β is the dipole tilt (10.4°). λ is independent of R and double valued unless $\delta=\beta$. The extent of the plasma sheet depends on solar aspect and is about 40 R_J in the subsolar direction, 90 R_J at -90°, 130 R_J at -115°, and 160 R_J at -137° from the subsolar point. This asymmetry is introduced by the solar wind pressure and is present in all models.

This simple model (Equation 3) applies close to Jupiter; however, as the observer moves further away, the values of λ were found to be larger than

predicted by Equation (3). This is equivalent to an R dependent twist of the plasma sheet about the rotational axis. The reason for the twist is a delay relative to the position of the magnetic equator (Northrop et al., 1976). Even if the magnetosphere were rigidly corotating, plasma moving radially away from Jupiter would load the field lines resulting in a B_ϕ component and field sweepback (Hill, 1980). Since the magnetotail configuration of the plasma sheet is much thinner and extends to greater radial distances than in the subsolar hemisphere, actual radial plasma motion has to occur when a given section of magnetosphere rotates from dusk to dawn. A lack of corotation would increase the sweep back. Field line slipping in the ionosphere, if it depends on latitude will also affect the delay. If the slippage increases with the latitude of the feet of the field lines, then this process will increase the delay; however, if slippage is more at some latitudes than others, we could also observe a relative phase advance.

In addition to the delay, the plasma sheet may be bent towards the plane of the ecliptic by solar wind pressure and towards the Joviographic equatorial plane by the centrifugal force on the (partially) corotating plasma. These features were incorporated in the model proposed by Kivelson (1978), which expressed the delay in terms of a finite radial velocity starting at a distance R_o. This model also permitted the local latitude of the plasma sheet to differ from that of the dipole. With these modifications, Equation (3) may be expressed as (Kivelson et al., 1978):

$$\lambda = \lambda_d \mp \cos^{-1} \frac{\tan \delta}{\tan \delta_o} + 36.27 \frac{(R-R_o)}{V} \quad \text{for } R > R_o \quad (4)$$

where δ_o is the local latitude of the plasma sheet, with the condition

$\delta \leq \delta_o \leq 10.4^o$, and V is a "velocity" produced by the various effects discussed above. Using Pioneer 10 data, Kivelson et al. (1978) found $\delta_o \approx \beta$ and V = 29 or 43 R_J/hr., depending on the criteria used in fitting the data.

Figure 11A shows an isometric projection of the plasma sheet plane described by Equation (3). The rigid disk in the dipole equator is illustrated with equally spaced concentric rings; the Z dimension has been multiplied by 3 to enhance the 10.4° tilts. The surface defined by equation 4 may be derived from this rigid disk. The effect of a finite V in equation 4 is to rotate the plane of each ring through an angle $\theta(R_1)$ around the spin axis, where θ stands for the last term in Equation (4). The effect of bending is to decrease the inclination of each ring from β to $\delta_o(R_1)$. The resulting surface is shown in figure 11B for an inclination of the outer ring of δ_o = 6.4° and a delay angle at the outer ring of $\theta = 50^o$. In figure 11B, the parameters δ_o, R_o and V are independent of λ; it should be noted, however, that this is not a necessary feature of this model.

If the spacecraft latitude is inserted for δ in Equations (3) or (4), then the two values of λ are the predicted longitudes of the plasma sheet crossings. The smaller λ refers to the leading crossing where the spacecraft goes from north to south of the plasma sheet, and the larger λ refers to the lagging crossing where the spacecraft emerges again to the north. If the spacecraft latitude δ is greater or equal to β, the plasma sheet approaches, but does not pass over, the spacecraft at longitude $\lambda = \lambda_d$. This was the geometry of the Pioneer 10 outbound trajectory. Since Voyagers 1 and 2 were close to a latitude of 5°, two crossings are expected out to a distance where $\delta_o \approx 5^o$.

We have used the peaks in the >0.4 MeV proton flux (Figures 4 and 5) to identify the center of the plasma sheet or our closest approach to it. For

this purpose, detailed plots were used as illustrated in Figure 12. If more than two peaks were present in a 10-hour period, the longitudes corresponding to the first and last peaks were used. Figure 12 also shows that for Voyager 2, double peaks persisted beyond 200 R_J, which is consistent with $\delta_o \approx \beta$, as determined from Pioneer 10. In order to determine the "velocity" in Equation (4), we have plotted in Figure 13 $\theta = \lambda_{III} - \lambda_d \pm \cos^{-1}(\tan \delta / \tan \delta_o)$ for $\delta_o = 10.4^o$, where θ is the angle illustrated in Figure 11, and is the difference between the longitude of maximum north excursion of the plasma sheet and λ_d, the longitude to which the dipole points in the southern hemisphere. Between 25 and 50 R_J, the slope of the Voyager 1 leading crossings differs from that of the lagging crossings (Table 5), and the delay was significantly longer for the leading than for the lagging crossings. For Voyager 2, the slopes are initially the same, but the two crossings have different delays beyond 50 R_J. For both missions at 100 R_J, the leading crossings were consistently delayed by 1 1/2 to 2 1/2 hours more than the lagging crossings. Such a result is consistent with our model, but requires different values of V at the two crossings. This led to the suggestion (Vogt et al., 1976b) that the average velocity has an azimuthal dependence which may be associated with the "active" and "inactive" hemispheres discussed by Vasyliunas (1975) and by Dessler (1978).

A different explanation for the apparent difference in delay of the two crossings is based on the bending of the neutral sheet towards the Jovigraphic equator; that is, δ_o becomes a function of R. Bending presumably was present during the Voyager 1 pass (Vogt, 1979a), because we often saw only one flux maximum for distances beyond 70 R_J, and did not actually cross the center of the plasma sheet (the magnetic field did not reverse, Ness et al., 1979a), even though Voyager 1 was at a latitude of only ~5°. If we assume equal

velocities, V, for the two crossings at a given R, Equation (4) can be solved for δ_o as, (Bridge et al., 1979):

$$\delta_o = \tan^{-1}(\tan \delta / \cos \tfrac{1}{2}\Delta\lambda) \quad (5)$$

Where $\Delta\lambda$ is the difference in longitude between the two crossings, and δ is the spacecraft latitude. The resulting maximum excursions of the plasma sheet ($Z = R \tan \delta_o$) are shown in Figure 14. Only Voyager 1 data were used between 20 and 70 R_J because the latitude of Voyager 2 was unfavorable. Beyond 80 R_J there was a distinct difference in the plasma sheet excursions between the two missions. For Voyager 1, it was mostly at, or just below, the spacecraft trajectory; while it was generally above the trajectory during the Voyager 2 outbound pass. The approximate neutral sheet positions shown in Figure 14 are in good agreement with the results of Bridge et al. (1979) who obtained a value of 5 ± 1^o from the combined Voyager 1 and 2 data.

The smooth curves for Voyager 1 and 2 plasma sheet excursions in Figure 14 are eyeball fits through the experimental points. Both Voyager 1 and 2 curves start with a slope of 10.4^o, bend over at 30 R_J and follow the Voyager 1 data to 70 R_J. For Voyager 1, δ_o is smoothly interpolated to $\sim 5.3^o$ at 150 R_J, where the maximum plasma sheet excursion becomes tangent to the spacecraft trajectory. The Voyager 2 data are tangent to $\delta_o = 6^o$ at 150 R_J. Our data set was reanalyzed with these values of δ_o; the results are shown in Figure 15 and summarized in Table 5. Since equal velocities at the two crossings is a basic assumption of the model, its success can be judged on whether or not the leading and lagging crossings have the same delay versus distance. As can be seen from Figure 15, the organization of the data is exceedingly good between 20 and 55 R_J and reasonable between 70 and 150 R_J. Between 55 and 70 R_J,

however, significant differences remain. It is exactly in this region that we observed particle acceleration during the Voyager 1 mission (59 R_J), and the discrepancy may be due to a relatively unstable plasma sheet configuration. A change in wave velocity between 55 and 70 R_J can be seen in both Figures 13 and 15; a significantly lower wave velocity is found inside 55 R_J than outside 70 R_J (Table 5).

The bent twisted disk model can account for the timing of the primary flux maxima; however, it cannot account for the observed fine structure in the data. Beyond 40 R_J, we frequently observed three pronounced peaks on both missions (Figures 4, 5 and 12) At larger distances this could easily be due to flapping of the plasma sheet in response to changes in the solar wind. This explanation, however, is inadequate at ~40 R_J when Voyager 2 was at a latitude of only 1.6°, compared to 9° for the plasma sheet (Fig. 14). Based on magnetic field data, the two main maxima were associated with plasma sheet crossings, but the smaller middle peak was not. The observation of these secondary peaks by both missions in association with approximately the same longitude ($\lambda_{III} \approx 40^\circ$) is most easily explained by an azimuthal asymmetry. It is doubtful that the intermediate peak is due to particle acceleration and injection onto higher magnetic latitude field lines because the flux was nearly isotropic (Fig. 12) and the energy spectrum did not change (Fig. 7). This leaves two possible explanations: A longitude-dependent tilt of the plasma sheet such that δ_o is smaller at $\lambda_{III} \approx 40^\circ$ than at the plasma sheet crossings which occurred at $\lambda_{III} \approx 300^\circ$ and 100°, respectively. The other explanation is based on a change in the thickness of the plasma sheet. If near $\lambda_{III} = 40^\circ$, it has the same latitudinal extent as in the subsolar hemisphere, then the flux would decrease more slowly with latitude than at other longitudes.

The Electron Clock

Although the above discussion was based primarily on the modulation of protons, energetic electron fluxes are also confined to the neighborhood of the plasma sheet (Figs. 4 and 5), and are subject to a similar modulation pattern. The region where the disk model is valid extends from 15 R_J out to about 40 R_J in the subsolar hemisphere, to 80 R_J at 5 A.M. local time (Pioneer 10), 120 R_J at 4 A.M. (Voyager 1) and 160 R_J at 2:30 A.M., as observed with Voyager 2. Beyond these distances, the flux changes of protons and low-energy elecrons become more irregular, while electrons above 8 MeV tend to show a 10-hour modulation. At all local times that were observed by Pioneers 10 and 11, minima occurred simultaneously in the high-energy electron flux (>8 MeV) when the longitude range $\lambda_{III} = 240^o$ to 310^o passes the subsolar point. This feature was originally pointed out by McKibben and Simpson (1974; also Simpson et al., 1975; for a more recent discussion, see Fillius and Knickerbocker, 1979) and extended to Jovian electrons in the magnetosheath and interplanetary space near Jupiter by Chenette et al. (1974; see also Smith et al., 1976). This in-phase modulation in widely different regions is referred to as the "clock" model.

The Voyager encounters 5 years later offered the first opportunity to re-examine the "clock" modulation and to test the presumption that the release mechanism depends on the solar aspect of a certain Jovian longitude. Ten-hour modulation of the >8 MeV electron flux in the subsolar hemisphere was observed with Voyager 2 between 40 and 60 R_J (Vogt et al., 1979b). The dominant magnetic field component pointed in the -Z direction (south), rather than radial, as in the disk region (inside 40 R_J). Three deep flux minima occurred

at subsolar longitudes λ_{III} = 306, 255 and 310°, consistent with clock model predictions. In contrast to Pioneer 10, the Voyager spacecraft entered the Jovian magnetosphere in the northern hemisphere, which introduced a 180° phase shift in the disk model. As a result, the disk model would predict that flux minima should occur at a local λ_{III} = 260° and a subsolar longitude, λ_{III}=240°. This is based on the dipole direction and a 60° phase lag at 60 R_J observed during the outbound pass (Fig. 15). Although the time of occurrence is essentially the same for both models, we believe that we were observing clock model modulation because of the indications that a well-organized plasma sheet did not exist in this region during the Voyager 2 encounter (Ness et al., 1979b).

The "clock" model modulation was observed during the outbound passes of Voyagers 1 and 2. Figure 16 shows Voyager 2 data (1 hr. averages) on the modulation of 2.6- to 5.1-MeV and 8- to 12-MeV electron fluxes both in the disk and clock regions. Also shown is the flux ratio between these two channels. As Chenette et al. (1974) have shown, this ratio reflects more accurately the "clock" modulation than the total electron flux. A characteristic feature of this modulation is a minimum in the electron flux above 6 MeV and, therefore, a periodic softening of the spectrum when λ_{III}=240° is near the subsolar point. The left panel of Figure 16 (118-140 R_J) reflects the strong intensity modulation observed in the disk region. Neither the flux minima nor the softest spectra occur at the predicted time, and the softest spectra occur closer to flux maxima. In the right panel of Figure 16 (194-225 R_J) the intensity modulation is smaller, softer spectra are observed at minimum flux and the timing of softest spectra coincides with clock model predictions. It is very significant that this feature persists in the magnetosheath region. Clearly the magnetopause does not constitute a

boundary to electrons which are controlled by the processes producing the clock model modulation. Apparently, the modulation holds for several consecutive cycles; however, departures occur, such as at 0400 on 7/27 in Figure 16.. As yet, we have no basis for attributing these deviations from the clock model to the solar winds, as opposed to internal changes in the Jovian magnetosphere.

To investigate the modulation over more extended periods, we performed an epoch analysis using the synodic period of Jupiter (9.2587 hrs.). Averages over 16 minute intervals were placed into an 18 bin histogram based on the λ_{III} of the subsolar point at the time of observations. Since interplanetary modulation also affects our observations, the epoch analysis was repeated using periods of 8.5 and 11.5 hrs. Based on the χ^2 test, we found in most cases analyzed that both the fluxes and flux ratios depended significantly on phase. The flux ratio results were the most consistent. The upper plot in Figure 17 shows a histogram covering the time during which Voyager 2 was in the boundary or sheath region near the magnetopause (162-279 R_J). Data from 0-120° have been repeated between 360 and 480°. The χ^2 value for 17 degrees of freedom was 2100 for the Jovian period and 750 or less for the other periods. Data gathered during 44 days about 3 months after encounter are shown in the lower panel of Figure 17. The χ^2 value was again significantly greater for the correct period (230 as compared to 118 or less, 17 degrees of freedom). Both graphs in Figure 17 confirm clock model modulation; however the degree of modulation is less at the later time.

Voyager 2 data from 3 months pre encounter and 4 months past encounter have been analyzed. The pre-encounter results (April-June 1979) and post-encounter results for September 13 to 26 1979 were less conclusive. The modulation was less and the χ^2 value for the Jovian period was not

siginficantly different from that for 8.5 or 11.5 hrs. Further analysis will be required to positively eliminate or identify clock model modulation during these times. However, our analysis to date confirms the modulation of the interplanetary electron flux by the Joviographic longitude relative to the Jupiter-Sun line. This modulation is time dependent and possibly depends also on spacecraft position relative to Jupiter.

Dessler and Hill (1975 and 1979) and Hill and Dessler (1976) proposed the magnetic anomaly model to explain the 10-hour modulation of the interplanetary electron flux. In this model, the plasma density is enhanced in an "active" hemisphere due to an increase in the ionospheric conductivity which is produced by precipitating electrons at a magnetic anomaly between $\lambda_{III} = 200$ to 270º (Acuna and Ness, 1976). It was postulated that this enhancement is not confined to the inner magnetosphere (L~6) and would play a particularly important role in the magnetotail where the solar wind pressure is removed. The denser plasma would escape along the tail and thus permit the escape of the trapped electrons.

In principal the expansion could proceed to infinity since many observations have demonstrated that the plasma pressure in the plasma sheet is at least equal to the magnetic field pressure. The expansion velocity, however, can be at most as high as the wave velocity we deduced from the plasma sheet crossings (Table 5), but it may actually be considerably lower because plasma motion is only one component of the wave speed. If the tail corotates, then only 4 to 5 hours are available and the expansion can proceed at most from 40 to 250 R_J, and is probably less. At that time the expanding trapped particle region would contact the dawn magnetopause in the region where the Pioneer 10 and Voyager trajectories crossed it (Fig. 2). It is, therefore, most likely that a major fraction of the release of energetic

electrons occurs there, or characteristically at approximately 100 R_J near the dawn meridian where the plasma either escapes or is recompressed. In the diffusion-convection model of interplanetary propagation (Pyle and Simpson, 1977; Chenette, 1980), observations of Jovian electrons near 1 AU are consistent with a release point close to Jupiter. Other investigators have interpreted the 1 AU data to imply a release point much further away from Jupiter (e.g. Krimigis et al., 1975; Pressos and Goertz, 1976); but under that interpretation, we may be dealing with two different populations (Pressos and Goertz, 1976). If the release is near the dawn meridian, we can estimate the longitude from which the anomalously soft electron spectrum originates. A subsolar longitude of 240° to 310° corresponds to a dawn meridian of 330° to 400°. The longitude responsible for the anamoly, however, passed the dawn meridan earlier, because of the propagation delay from the inner magnetosphere to the magnetopause and any electron drift. According to Figures 13 and 15, the delay is between 70° and 100°. The curvature and gradient drifts must be small because there is no consistent separation between flux minima for 2 and 8 MeV electrons. Because of the highly-distorted field configuration, we have not calculated maximum drift angles consistent with our data, but we estimate that 50° constitutes a conservative upper limit. This would place the longitude responsible for the low electron flux into the range of λ_{III} = 180° to 330°, which brackets the longitude of the magnetic anomaly.

Azimuthal asymetries in the electron population will separate with time because gradient and curvature drifts are energy dependent. The in-phase modulation of the 2 and 8 MeV flux implies either a short residence time in the magnetosphere or modulation at the release point. The fact that the modulation is observed inside, as well as outside, the magnetosphere would favor the former explanation. This is also consistent with the observation

that Jupiter injects into interplanetary space in 10 hours a number of electrons comparable to the content of the outer magnetosphere (Fillius et al., 1977). One would expect that the release of electrons across the magnetopause and local acceleration becomes more probable as the plasma loading increases in the boundary region near the magnetopause. Yet we find that the minimum in the electron flux is apparently associated with the active hemisphere which presumably has the higher plasma density. We propose that relatively small differences in the "wave velocity" discussed in the last section could produce a minimum in plasma loading and, hence, the required modulation (Vogt et al., 1979b). Although the most plausible plasma sheet model, the bent twisted disk, does not involve a longitudinal dependence of the "wave velocity," such differences may still exist at the required longitude to produce the clock modulation. In any case, the fine structure in the data clearly requires some azimuthal asymmetry. Figure 18 illustrates stream lines vs. radial distance and λ_{III} as they would appear to an observer in the dawn meridian. Note that an observer on the subsolar meridian would see a somewhat different picture because the magnetopause is not symmetric. A difference in expansion velocity was introduced between the active and inactive hemispheres with the transition from the inactive to the active hemisphere at $\lambda_{III} = 240^{o}$. With a slower expansion velocity in the active hemisphere, a rarefaction region will develop at this boundary, which arrives at the dawn magnetopause when $\lambda_{III} = 240^{o}$ is at the subsolar point. This small region should have a lower plasma density than either the active or inactive hemispheres, and it is precisely this sharp minimum which is the characteristic of the clock model. It is also evident from Fig.1 and 18 that Voyager during its inbound trajectory (40 to 60 R_J) would encounter the rarefaction region at about the same subsolar longitude. A flux maximum would

be expected when the transition from the active to inactive hemisphere reaches the dawn magnetosphere.

The magnetodisk crossings during the outbound passes of Voyager occurred primarily between the two solid stream lines (Fig. 18) which start at λ_{III} = 330 and 90°. With a 10.4° disk, all crossings would have been near these lines; with a bent disk, they would have occurred mostly near the center of this region. Since the available data come from only one hemisphere and were not taken near the interesting region for the clock model, we can only argue that the proposed model is plausible. To resolve this question, we need plasma sheet crossings in the southern hemisphere and near the dawn meridian.

Summary and Conclusions

The Jovian magnetotail at solar aspect angles between 90° and 140° in the dawn direction possesses a thin plasma sheet whose effects have been observed out to 160 R_J. Trapped energetic electrons (0.3 to 12 MeV) and protons (0.4 to 8 MeV) are confined to this disk to within a few degrees in latitude. In the tail lobe, interplanetary protons above 2 MeV were already encountered at 42 R_J only 15° above the disk and were found considerably closer to the disk at greater distances. This is taken as strong evidence that these field lines are open and thus would facilitate the escape of energetic particles which reach them through a process like cross field diffusion.

The well-organized plasma sheet appears to break down near the magnetopause. The disappearance of the plasma disk is particularly noticable in the modulation of the electron flux (Figure 5). At a distance of about 15 R_J inside the magnetopause, the electron flux increased to its prior value in the plasma sheet and remained that high even in the sheath region outside the magnetopause. Intensity changes became smaller and less regular. The region inside the magnetopause appears to be a boundary layer. Gurnette et al.

(1980) identified the boundary layer by the enhanced population of thermal electrons; however, the boundary layer defined by thermal electrons appears to be thicker. For instance, during the Voyager 1 outbound pass Gurnette et al.(1980) observed the thermal electron boundary layer starting at 100 R_J, while the boundary layer for energetic electrons starts at 135-145 R_J.

Comparable proton fluxes were observed in the plasma sheet by Voyager 1 and 2. The flux > 0.4 MeV protons decreased by about three orders of magnitude from 20 to 90 R_J and then remained relatively constant. The flux increased again by almost an order of magnitude in the boundary layer, at least if the boundary had been compressed recently. In the plasma sheet and boundary layer, the spectrum is best represented by an exponential in rigidity with a characteristic energy of 50 ± 30 keV. Proton spectra agree with interplanetary spectra in the tail lobe (E_0 > 500 keV), become quite soft as the plasma sheet is approached (E_0 ~ 20 keV) and then harder again (E_0 ~ 50 keV) at the center of the plasma sheet. The plasma sheet in the tail is quite active; both proton acceleration and field aligned streaming have been observed. Under these conditions both energy spectra and intensities can depend sensitively on direction relative to the magnetic field.

During most of the outbound passes of Voyagers 1 and 2, proton and electron modulation tracked each other closely. There is a tendency for the electron flux to show less of a dip than protons between two closely spaced neutral sheet crossings or approaches. Most flux changes observed in 2- and 8-MeV electrons were in phase; thus the lack of differential drift indicated local effects. In the region of disk model control, the electron spectrum from 2 to 12 MeV was softer near maximum flux, i.e. near the plasma sheet. This relation was reversed in the boundary layer and, outside the magnetopause, in the sheath and interplanetary space, where the clock model applies. It should be noted, however, that modulation of the intensities and

spectra in this region was not nearly as consistent as inside 140 R_J.

The Pioneer 10 and 11 missions established (Smith et al., 1974) that a well developed current sheet exists near the magnetic equator inside of 40 R_J in the dawn direction. The Pioneer 11 outbound pass indicated that the trapping region is thicker near the subsolar meridian than at ~ 30° from the Jupiter-Sun line. Between 20 and 30 R_J in the antisolar direction, Voyager 2 observed an energetic particle population which covered almost as large a latitudinal extent as was observed at -30° from the subsolar direction and not nearly as thin as at a solar aspect of -90°. It is doubtful that this large an effect is due to temporal changes, and we believe this observation furnishes evidence that the magnetospheric plasma does indeed expand into the tail, but because of the finite velocity the expansion had just barely affected the plasma sheet from 20 to 35 R_J near the antisolar direction.

The many approaches to and crossings of the plasma sheet by Pioneer 10 and Voyagers 1 and 2 give plasma sheet positions at several latitudes and longitudes. These positions can be compared to predictions by models of the plasma sheet configuration in an attempt to gain an overall description of the plama sheet. Various interpretations based upon Voyager data have been published by Bridge et al. (1979), Carbary (1980), Ness et al. (1979b), Vogt et al. (1979a,b) and Vasyliunas and Dessler (1980). Most of these authors used the model described by Kivelson et al. (1978) which involves twisting the dipole equator through an angle θ(R) around the Jovian spin axis, and the possibility of bending it as a function of distance towards the Jovigraphic equator (Fig. 21). In this paper, "twisted disk" refers to a model with the plasma sheet at a constant latitude of 10.4°, and "bent twisted disk" allows the latitude to decrease, as a function of distance, to values below 10.4°.

From this analysis we conclude that the Voyager 2 data, with generally

two crossings for each Jovian period, are consistent with both the twisted disk and bent twisted disk models. For the simple twisted disk, the angle of rotation depends not only on radius but also on longitude, as first pointed out by Vogt et al. (1979b). The implications of this model are described in more detail by Vasyliunas and Dessler (1980). Results from both missions taken together favor the bent twisted disk not only because of the absence of Voyager 1 neutral sheet crossings beyond 80 R_J, but also because Voyager 2 observed essentially the same wave velocity between 30-55 R_J at both crossings, while Voyager 1 found a significant difference in this region (Fig. 13 and Table 5). Because of the difference between the two trajectories (Fig. 14) this is exactly what would be expected from a bent twisted disk in the absence of azimuthal asymmetry. Between 30 and 60 R_J, our results with the bent twisted disk agree with Bridge et al. (1979). Our results differ from the model identified by Carbary (1980) as "Wavy II" in that the maximum plasma sheet excursion in his model reaches a fixed amplitude while our results require that the maximum excursion grows as $\sim R \tan 6^o$. One feature of the bent twisted disk model is that different amounts of bending are required to fit data from the three missions; no or little bending was present during the Pioneer 10 pass, bending from 10.4° to 6° for Voyager 2 and to 5° for Voyager 1. Changes in the plasma loading in the magnetosphere should affect the departure of the plasma sheet from the dipole equator. Since temporal changes are known to occur, it is quite possible that the amount of bending was different for each mission.

A new result of our detailed analysis is the finding that the wave speed changes significantly between 50 and 70 R_J (Fig. 13 and 15). This was not realized by the other investigators and explains why quite different wave speeds can be obtained depending on the exact range over which the data are

fit. Magnetic perturbations propagate with the Alfven group velocity along field lines, and Kivelson et al. (1978) and Carbary (1980) have equated the wave velocity discussed above with the Alfven velocity. A comparison between the wave velocities derived from the three missions and the corotation velocity is shown in Figure 19. A general criterion for corotation is that the Alfven velocity exceeds the corotation velocity. If taken literally, Figure 19 shows that corotation should cease near 30 R_J but become possible again beyond 70 R_J. However, the interpretation of the wave velocity as an Alfven velocity has not been firmly established, and in the model of Northrop et al. (1974) no such association can be made.

The bent twisted disk model accounts for the overall plasma sheet location; however, the additional flux peaks observed by both Voyagers between 40 and 60 R_J are difficult to explain without a λ_{III} dependent asymmetry. Such an asymmetry is also required by the "clock" modulations of electrons in the outer magnetosphere and interplanetary space.

The degree of corotation of the plasma sheet in the magnetotail is very important because it determines whether the Jovian plasma escapes down the tail or piles up at the dawn magnetopause in a boundary layer. In the latter case, a part of this boundary layer would still escape along the tail, but a substantial fraction should continue to rotate with Jupiter and be recompressed to form a thick boundary layer in the subsolar hemisphere. As yet no consistent picture has emerged from the experimental evidence. The lack of complete corotation between 20 and 45 R_J in the subsolar hemisphere was demonstrated from plasma data by McNutt et al. (1979; see also McNut and Belcher, 1980). Analysis of the first order anisotropy in the energetic proton flux ($E > 0.5$ MeV) has been the other major source of data on corotation. However, first order anisotropies have to be corrected for flux

gradients and higher order anisotropies (Northrop and Thomsen 1980), resulting in a significant reduction in the accuracy with which the corotation velocity can be determined. On this basis McDonald et al. (1979) found that corotation was not present beyond 70 R_J in the subsolar hemisphere (Pioneer 10). Carbary et al. (1980) have interpreted their Voyager data to imply that much of the magnetosphere is relatively close to corotation. Our preliminary analysis of Voyager 1 observations in the tail is consistent with corotation even at 100 R_J.

It would appear that the degree of corotation must be subject to significant temporal as well as spatial variations. For instance a major injection of gas from Io would significantly slow down corotation in the torus region and affect the outer magnetosphere only later. The neutralization of ions in the torus region discussed by Eviatar et al. (1976) permits escape of neutrals from the inner magnetosphere without affecting the outer magnetosphere. Corotation determines the extent to which Jupiter's angular momentum is coupled to the magnetosphere and therefore plays a key role in the energetics of the whole magnetosphere; it is particularly significant towards understanding the dawn magnetosphere.

The Voyager missions confirmed the "clock" model modulation (Chenette et al., 1974) of the Jovian electron flux just outside the magnetopause and in the boundary layer. A large phase shift occurred in the 8-MeV electron flux between the region where disk model modulation dominated and the outer region. Surprisingly enough, the phase of the softest electron flux did not change. Softer spectra were found near maximum flux in the disk model region and near minimum flux in the clock model region.

In trying to understand the modulation of the electron flux and spectrum in the boundary layer and magnetosheath, we have assumed a substantial degree

of corotation. Some electrons presumably diffuse onto open field lines and escape throughout the tail region; however, a major release point should be near the dawn magnetopause. In this region the corotating plasma should form a thick boundary layer and a relatively unstable magnetopause. If this holds true, then the electron modulation can be associated with the active hemisphere and, when account is taken of the propagation delay, minimum flux corresponds to a subsolar longitude, $\lambda_{III} \sim 240^{\circ}$. This type of modulation clearly requires a longitudinal asymmetry, and we suggest that a region with the least amount of plasma loading would arrive at the dawn magnetopause at the appropriate phase if a separation occurred at the boundary between the active and inactive hemispheres. This should be observable as a difference in the wave velocity and may be due to a somewhat greater departure from corotation in the active hemisphere. Unfortunately the available data are inconclusive on this point, and additional observations are required in the southern hemisphere and at more favorable longitudes.

Acknowledgments

The authors are indebted to the Voyager magnetometer team headed by N.F. Ness for permission to use their magnetic field data; R.P. Lepping was particularly helpful in preparing the data. T. Conlon's and N. Lal's participation in the early phases of the data analysis and discussions with T.G. Northrop are gratefully acknowledged. This work would have been impossible without the close collaboration and assistance from the CRS team members and collaborators at the California Institute of Technology.

REFERENCES

Acuna, M. H. and N. F. Ness, Results from the GSFC Fluxgate Magnetometer on Pioneer 11, in Jupiter, edited by T. Gehrels, p. 830, U. of Arizona Press, Tucson 1976.

Birmingham, T. J. and T. G. Northrop, Theory of Flux Anisotropies in a Guiding Center Plasma, J. Geophys. Res. 84, 41, 1979.

Bridge, H. S., J. W. Belcher, A. J. Lazarus, J. D. Sullivan, F. Bagenal, R. L. McNutt, Jr., K. W. Ogilvie, J. D. Scudder, E. C. Sittler, V. M. Vasyliunas, and C. K. Geortz, Plasma Observations Near Jupiter: Initial Results from Voyager 2, Science 206, 972, 1979.

Burlaga, L. F., J. W. Belcher, and N. F. Ness, Disturbances Observed Near Ganymede by Voyager 2, Geophys. Res. Lett. 7, 21, 1980.

Carbary, J. F., Periodicities in the Jovian Magnetosphere: Magnetodisk Models after Voyager, Geophys. Res. Lett. 7, 29, 1980.

Carbary, J. F., S. M. Krimigis, E. P. Keath, G. Gloeckler, W. I. Axford, and T. P. Armstrong, Ion Anisotropies in the Outer Jovian Magnetosphere, J. Geophys. Res. to be published 1980.

Chenette, D. L., T. F. Conlon, and J. A. Simpson, Bursts of Relativistic Electrons from Jupiter Observed in Interplanetary Space with the Time Variation of the Planetary Rotation Period, J. Geophys. Res. 79, 3551 1974.

Chenette, D. L., The Propagation of Javian Electrons to Earth, J. Geophys. Res. 85, 2245, 1980.

Conlon, T. F., A. W. Schardt, F. B. McDonald, J. H. Trainor, and N. Gehrels, The Detection of Interplanetary Protons Deep in Jupiter's Magnetosphere, EOS 60, 919, 1979.

Dessler, A. J., Longitudinal Control of Jovian Magnetopause Motion, Geophys. Res. Lett. 5, 65, 1978.

Dessler, A. J. and T. W. Hill, Jovian Longitudinal Control of Io-Related Radio Emissions, Ap. J. 227, 664, 1979.

Dessler, A. J. and T. W. Hill, High-Order Magnetic Multipoles as a Source of Gross Asymmetry in the Distant Jovian Magnetosphere, Geophys. Res. Lett. 2, 567, 1975.

Eviatar, A., Y. Mekler, and F. V. Coroniti, Jovian Sodium Plasma, Astrophys. J. 205, 622, 1976.

Fillius, W. and P. Knickerbocker, The Phase of the Ten-Hour Modulation in the Jovian Magnetosphere (Pioneer 10 and 11), J. Geophys. Res. 84, 5763, 1979.

Fillius, W., Wing-Huen Ip and P. Knickerbocker, Interplanetary Electrons: What is the Strength of the Jupiter Source?, 15th International Cosmic Ray Conference, Plovdiv, Bulgaria, 1977.

Frank, L. A., K. L. Ackerson, and R. P. Lepping, On Hot Tenuous Plasmas, Fireballs, and Boundary Layers in the Earth's Magnetotail, J. Geophys. Res. 81, 5859, 1976.

Gleeson, L. J. and W. I. Axford, An Analytic Model Illustrating the Effects of Rotation on a Magnetosphere Containing Low-Energy Plasma, J. Geophys. Res. 81, 3403, 1976.

Goertz, C. K. and M. F. Thomsen, The Dyanmics of the Jovian Magnetosphere, Rev. Geophys. and Space Sci. 17, 731, 1979.

Goertz, C. K., The Current Sheet in Jupiter's Magnetosphere, J. Geophys. Res. 81, 3368, 1976.

Goertz, C. K., D. E. Jones, B. A. Randall, E. J. Smith, and M. F. Thomsen, Evidence for Open Field Lines in Jupiter's Magnetosphere, J. Geophys. Res. 81, 3393, 1976.

Gurnett, D. A., W. S. Kurth, and F. L. Scarf, The Structure of the Jovian Magnetotail From Plasma Wave Observations, Geophys. Res. Lett. 7, 53, 1980.

Hill, T. W., Corotation Lag in Jupiter's Magnetosphere: Comparison of Observation and Theory, Science 207, 301, 1980.

Hill, T. W. and A. J. Dessler, Longitudinal Asymmetry of Jovian Magnetosphere and the Periodic Escape of Energetic Particles, J. Geophys. Rev. 31, 3383, 1976.

Ipavich, F. M., The Compton-Getting Effect for Low Energy Particles, Geophys. Res. Lett. 1, 149, 1974.

Kivelson, M. G., P. J. Coleman, Jr., L. Froideaux, and R. L. Rosenberg, A Time Dependent Model of the Jovian Current Sheet, J. Geophys. Res. 83, 4823, 1978.

Kivelson, M. G. and C. R. Wing, Field-Aligned Currents in the Jovian Magnetosphere: Pioneer 10 and 11, J. Geophys. Res. 81, 5853, 1976.

Krimigis, S. M., T. P. Armstrong, W. I. Axford, C. O. Bostrom, C. Y. Fan, G. Gloeckler, L. J. Lanzerotti, D. C. Hamilton, and R. D. Zwickl, Energetic (~ 100-keV) Tailward-Directed Ion Beam Outside the Jovian Plasma Boundary, Geophys. Res. Lett. 7, 13, 1980.

Krimigis, S. M., T. P. Armstrong, W. I. Axford, C. O. Bostrom, C. Y. Fan, G. Gloeckler, L. J. Lanzerotti, E. P. Keath, R. D. Zwickl, J. F. Carbary, D. C. Hamilton, Hot Plasma Environment at Jupiter: Voyager 2 Results, Science 206, 977, 1979.

Krimigis, S. M., E. T. Sarris, and T. P. Armstrong, Observations of Quiet Time Interplanetary Electron Enhancements of Jovian Origin, Geophys. Res. Lett. 2, 561, 1975.

Lupton, J. E. and E. C. Stone, Measurement of Electron Detection Efficiencies in Solid-state Detectors, Nucl. Instr. and Meth. 98, 189, 1972.

McDonald, F. B., A. W. Schardt, and J. H. Trainor, Energetic Protons in the Jovian Magnetosphere, J. Geophys. Res. 84, 2579, 1979.

McKibben, R. B., J. A. Simpson, Evidence From Charged Particle Studies for the Distortion of the Jovian Magnetosphere, J. Geophys. Res. 79, 3545, 1974.

McNutt, R. L. and J. W. Belcher, Positive Ion Observations in the Middler Magnetosphere of Jupiter, J. Geophys. Res., this issue, 1980.

McNutt, R. L., Jr., J. W. Belcher, J. D. Sullivan, F. Bagenal, and H. S. Bridge, Departure From Rigid Co-rotation of Plasma in Jupiter's Dayside Magnetosphere, Nature 280, 803, 1979.

Ness, N. F., M. H. Acuna, R. P. Lepping, L. F. Burlaga, K. W. Behannon, and F. M. Neubauer, Magnetic Field Studies at Jupiter by Voyager 1: Preliminary Results, Science 204, 982, 1979a.

Ness, N. F., M. H. Acuna, R. P. Lepping, K. W. Behannon, L. F. Burlaga, and F. M. Neubauer, Jupiter's Magnetic Tail, Nature 280, 799, 1979b.

Northrop, T. G. and M. F. Thomsen, Theory of Flux Anisotropies in Saturn's Magnetosphere, to be published in J. Geophys. Res. 1980.

Northrop, T. G., C. K. Goertz, and M. F. Thomsen, The Magnetosphere of Jupiter as Observed with Pioneer 10, 2, Nonrigid rotation of the Magnetodisc., J. Geophys. Res. 79, 3579, 1974.

Presses, M. E. and C. K. Goertz, Jupiter's Magnetotail as the Source of Interplanetary Jovian MeV Electrons Observed at Earth, Geophys. Res. Lett. 3, 228, 1976.

Pyle, K. R. and J. A. Simpson, The Jovian Relativistic Electron Distribution in Interplanetary Space From 1 to 11 AU: Evidence for a Continuously Emitting "Point" Source, Ap. J. 215, L89, 1977.

Sarris, E. T., S. M. Krimigis, and T. P. Armstrong, Observations of Magnetospheric Bursts of High-Energy Protons and Electrons at ~ $35R_E$ with IMP 7, J. Geophys. Res. 81, 2341, 1976.

Simpson, J. A., D. C. Hamilton, G. A. Lentz, R. B. McKibben, M. Perkins, K. R. Pyle, A. J. Tuzzolino, and J. J. O'Gallagher, Jupiter revisted: First results from the University of Chicago Charged Particle Experiment on Pioneer 11, Science 188, 455, 1975.

Smith, E. J., B. T. Tsurutani, D. L. Chenette, T. F. Conlon, and J. A. Simpson, Jovian Electron Bursts: Correlation With the Interplanetary Field Direction and Hydromagnetic Waves, J. Geophys. Res. 81, 65, 1976.

Smith, E. J, L. Davis, D. E. Jones, P. J. Coleman, Jr., D. S. Colburn, P. Dyal, C. P. Sonett, and A. M. A. Frandsen, Planetary Magnetic Field and Magnetosphere of Jupiter: Pioneer 10, J. Geophys. Res. 79, 3501, 1974.

Stone, E. C., R. E. Vogt, F. B. McDonald, B. J. Teegarden, J. H. Trainor, J. R. Jokipii, and W. R. Webber, Cosmic Ray Investigation for the Voyager Mission: Energetic Particle Studies in the Outer Heliosphere - and Beyond, Space Sci. Rev. 21, 355, 1977.

Vogt, R. E., W. R. Cook, A. C. Cummings, T. L. Garrard, N. Gehrels, E. C. Stone, J. H. Trainor, A. W. Schardt, T. Conlon, N. Lal, and F. B. McDonald, Voyager 1: Energetic Ions and Electrons in the Jovian Magnetosphere, Sci. 204, 1003, 1979a.

Vogt, R. E., A. C. Cummings, N. Gehrels, E. C. Stone, J. H. Trainor, A. W. Schardt, T. F. Conlon, and F. B. McDonald, Voyager 2: Energetic Ions and Electrons in the Jovian Magnetosphere, Sci, 206, 984, 1979b.

Van Hollebeke, M. A. I., F. B. McDonald, J. H. Trainor, and T. T. von Rosenvinge, Energy Spectrum of Energetic Particle Streams in the Inner and Outer Solar System, Bull. Am. Phys. Soc. 23, 509, 1978.

Vasyliunas, V. M. and A. J. Dessler, The Magnetic Anomaly Model of the Jovian Magnetosphere: A Post Voyager Assessment, J. Geophys. Res., this issue, 1980.

Vasyliunas, V. M., Modulation of Jovian Interplanetary Electrons and the Longitude Variation of Decimetric Emission, Geophys. Res. Lett. 2, 87, 1975.

TABLE 1

	Spacecraft Longitude from Subsolar Point At: 20 R_J	50 R_J	100 R_J	150 R_J	Distance at Magnetopause Crossing (R_J)
Voyager 2	177	-150	-140	-137	170-280
Voyager 1	-140	-123	-118	-115	158-165
Pioneer 10	-107	- 95	- 90	- 87	97-150

TABLE 2

CRS DETECTORS USED DURING JUPITER ENCOUNTER

Detector	Shielding	Energy Range+ (MeV)	Factor (cm^2 ster)	Comments
Protons (LET)				
L1*	0.8 mg/cm^2 Al	0.42 – 12	4.8	Also, Alphas above 0.32 MeV/n
L2*	8.1 mg/cm^2 Si	1.8 – 13	0.43	Through L1
	>140 mg/cm^2 Al	>9	8.4	Protons through side comparable to those through front for E^{-2} spectrum
L1 L2 $\overline{L4}$		1.8 – 8	0.43	ΔE – E analysis
L1 L2 L3 $\overline{L4}$		3 – 8	0.43	ΔE_1, ΔE_2 – E analysis
Electrons (HET)				
0.15 mm Si detector	0.9 mg/cm^2 Mylar		∿25	Responds primarily to 0.1–0.4 MeV electrons
Range 4 –10 mm Si	"	2.6 – 5.1	1.46	Coincidence rates with good background rejections, but accidental coincidence problems at high counting rates
10 – 16 mm Si	"	5.1 – 8	1.25	
16 – 22 mm Si	"	8 – 12	0.96	
Electrons (TET)				
D_1 (3 mm Si)*		>0.5 MeV	∿14	Usable at higher flux than HET rates
D_3 (3 mm Si)	∿1.2 cm Si equivalent	>5 MeV	∿14	" " " " " " "
Various Coincidence Combinations		2 to 50 MeV	3.1 to 0.66	

*Single Rates

+Small Difference Between Similar Detectors

TABLE 3

VOYAGER 1, COROTATION AND GRADIENT ANISOTROPIES

DISTANCE (R_J)	γ	$\rho_g \frac{\partial \ln J}{\partial z}$	LET A/LET D Predicted	LET A/LET D Observed	COMMENTS
34	3.3	-0.024	1.31	1.46	near flux maximum
50	1.3	-	1.21	1.06	near flux minimum
104	3.6	-0.116	2.4	2.1	near flux maximum
107	1.5	-	1.24	1.24	near flux minimum

TABLE 4

OBSERVATIONS OF PROTONS STREAMING AWAY FROM JUPITER

DOY	DATE	TIME	DISTANCE	
	VOYAGER 1			
70	3/11	500 to 700	98 R_J	Outward flow within 15° of magnetic field direction intensity ratio 0 to 90° pitch angles 40:1.*
72	3/13	1600 to 1830	133 R_J	Outward flow along B, intensity ratio 20:1.*
76	3/17	1100 to 1300	188 R_J	Outward flow from Jupiter in magnetosheath region, intensity ratio 2:1* (2-5 MeV electrons ratio 1.5).
	VOYAGER 2			
203	7/22	800 to 1200	155 R_J	Outward flow along swept back field directions, intensity ratio 20:1 for detectors not well aligned with field. This event was also observed at low energies (Krimigis et al., 1980).
207	7/26	1200 to 1600	200 R_J	Outward flow but less extreme than the 7/22 event.

*Intensity ratio of >0.41 MeV protons between LET B and LET A.

TABLE 5

Wave Velocity into the Magnetotail of the Neutra Sheet Position

Spacecraft	Range	10.4^{o} Tilted Disk		Bent Twisted Disk	
	(R_J)	$V(R_J/hr)$	$R_o(R_J)$	$V(R_J/hr)$	$R_o(R_J)$
Pioneer 10	17-85	35.5 ± 5.4	7 ± 9		
Voyager 1					
active	20-55	19 ± 2	22 ± 4	23 ± 4	21 ± 6
inactive	20-55	43^{+30}_{-13}	17 ± 17		
active	70-140	44^{+16}_{-9}	-------	63^{+21}_{-13}	-------
inactive	70-140	146^{+830}_{-67}	-------		
Voyager 2					
active	30-55	19 ± 2	34 ± 5	18.3 ± 1.5	35 ± 4
inactive	30-55	18 ± 2	35 ± 5		
active	70-140	107^{+2000}_{-52}		204^{+3000}_{-99}	-------
inactive	70-140	$716^{+\infty}_{-530}$			

FIGURE CAPTIONS

Figure 1. Jupiter encounter trajectories projected into the ecliptic plane for Pioneer 10 and Voyager 1 and 2. Tick marks were placed to indicate the start of a new day. The two magnetopause positions shown correspond to typical high and low solar wind pressures.

Figure 2. Schematic drawing of the Voyager LET instrument. The detectors are enclosed in an aluminum housing with an average thickness of 0.025 inches.

Figure 3. Orthographic projection of unit vectors representing the look directions of the four LET detectors (A, B, C, and D) during the outbound pass of Voyager 1. The ecliptic plane is within 3° of the Joviographic equator. The angles from the +R direction are $\phi_A = 304°$, $\phi_B = 165°$, $\phi_C = 124°$ and $\phi_D = 69°$, and the inclination angles are $\vartheta_A = 66°$, $\vartheta_B = 19°$, $\vartheta_C = -66°$, and $\delta_D = 16°$. The positions shown applied at 55 R_J and were within ± 15° from 30 R_J to the magnetopause.

Figure 4. Electron (2.6-5.1 MeV) and proton fluxes (16 minute averages) observed between 20 and 130 R_J during the outbound passes of Voyagers 1 and 2 towards -115° and -137°, respectively, from the Jupiter-Sun line. Electron and >1.8-MeV proton fluxes above $10^3/cm^2$ sec ster are uncertain because of large corrections and are plotted only to show relative trends. The proton fluxes were derived from averages of three LETs (A B D for Voyager 1 and A C D for Voyager 2).The electron flux is based on a triple coincidence channel of the HET covering electrons with ranges between 4 and 10 mm of Si.

Figure 5. The fluxes shown in Figure 4 are extended from 130 to 250 R_J. The shading near the distance scale indicates when the spacecraft were in the Magnetosheath.

Figure 6. Proton momentum spectra for 64 min. intervals observed during the outbound pass of Voyager 1. Spectra at 34.2, 59.0, 64.9, and 116.9 R_J were observed during plasma sheet crossings; the 42.4 R_J spectrum represents interplanetary particles observed 15° above the magnetic equator; and the 146 R_J spectrum shows the particle population observed prior to the first magnetopause crossing.

Figure 7. Result of least squares fit to 64 min. averages of the Voyager 1 LET A pulse height distributions. A differential spectrum of the form $j(E) = KE^{-1/2} \exp -\sqrt{E/E_o}$ was fit to the data; this is equivalent to $j(p) = K' \exp -p/p_o$. The top panel shows the differential flux at 1 MeV and the lower panel gives the characteristic energy, E_o.

Figure 8. Result of least squares fit to 15 min. averages of Pioneer 10 observations during the outbound pass. The top panel shows the proton counting rate in a detector with a geometric factor of 0.015 cm^2 ster, and the lower panel gives the characteristic energy for the same spectral fit as Figure 7.

Figure 9. Field aligned flow of protons with energies above 0.4 MeV away from Jupiter observed with Voyager 1 near 98 R_J. LET B is pointed anti-parallel to the field line towards the planet and LET A perpendicular to the field. The peak flux in LET B of 830 protons/cm^2 sec ster is about 40 times the flux observed at the other plasma sheet crossings near 100 R_J.

Figure 10. Proton momentum spectra averaged over 64 min. observed during the streaming event near 98 R_J. The spectrum of protons streaming along the magnetic field is characteristic of particles trapped near the neutral sheet. The near 90° pitch angle particles (LET A) have a spectrum similar to that observed in the acceleration event near 59 R_J.

Figure 11. Isometric projection of the neutral sheet position as described by the rigid disk model (Fig. 11A) and by a bent twisted disk (Fig. 11B). The disk is illustrated by equally-spaced concentric circles; the Z dimension has been multipled by 3 to enhance the $\beta = 10.4^{o}$ dipole tilt. $\theta(R)$ in Fig. 11A shows in the ecliptic plane the delay angle used in computing Figure 11B. In both figures the inclination of the two inner rings is 10.4^{o} but decreases to 6.4^{o} for the outer ring in Figure 11B.

Figure 12. Comparison of Voyager 2 plasma sheet crossings at various distances from Jupiter. LET A is indicated by x, LET C by □, and LET D by ●.

Figure 13. Change in plasma sheet crossing corrected for lead or lag relative to dipole tilt for a 10.4^{o} inclination of the plasma sheet. The angle plotted is $\lambda_{III} - 20.8 \pm \cos^{-1}(\tan \delta / \tan 10.4)$, where δ is the local spacecraft latitude. Solid circles refer to leading crossing or approaches in the active hemisphere and open circles to the lagging crossing or approaches.

Figure 14. Maximum excursion from the Jovigraphic equator or dipole equator ($R \tan 10.4^{o}$) and of bent disk ($R \tan \delta_{o}$). The Voyager trajectories are shown by dashed lines. The values for δ_{o} were derived from the Voyager 1 and 2 data under the assumption of equal wave velocity at the leading and lagging crossings.

Figure 15. Changes in plasma sheet crossings corrected for lead and lag relative to the bent disk shown in Figure 14. The angle plotted is $\lambda_{III} - 20.8^{o} \pm \cos^{-1}(\tan \delta / \tan \delta_{o})$ where δ is the spacecraft latitude. Solid circles refer to leading and open circles to lagging crossings or approaches.

Figure 16. Fluxes and relative intensities of 2.5- to 5- and 8- to 12- MeV electrons as observed with Voyager 2. Data from 7/19 to 7/21 (118 to 140

R_J) were taken in the disk modulation region and data from 7/26 to 7/29 (194 to 225 R_J) in the clock modulation region. Dashed lines correspond to time of softest spectra predicted by clock model (λ_{III} = 240° at the subsolar point).

Figure 17. Histogram of the ratio of low- (2.5-5 MeV) to high- (8-12 MeV) energy electron fluxes versus λ_{III} of the Jovian subsolar point. The upper panel gives Voyager 2 data accumulated in the boundary and sheath region near the magnetopause (162-279 R_J). The lower panel gives Voyager 2 post-encounter data averaged from September 29 to November 11, 1979.

Figure 18. Illustrations of plasma sheet stream lines vs. radius for different velocities in the active and inactive hemispheres. The following radial velocities were used for this illustration: active hemisphere, 20 R_J/hr. to 65 R_J and 50 R_J/hr. 65 to 150 R_J; inactive hemisphere, 50 R_J/hr. Notice the rarefaction region at transition from inactive to active hemispheres and the enhanced flux region at transition from inactive to active hemisphere. Solid stream lines gives approximate positions of neutral sheet crossings for twisted disk (10.4° inclination).

Figure 19. Jovian corotation velocity vs. distance. The rectangles give the wave velocities and their uncertainties (Table 5) derived with the bent twisted disk model for the plasma sheet positions.

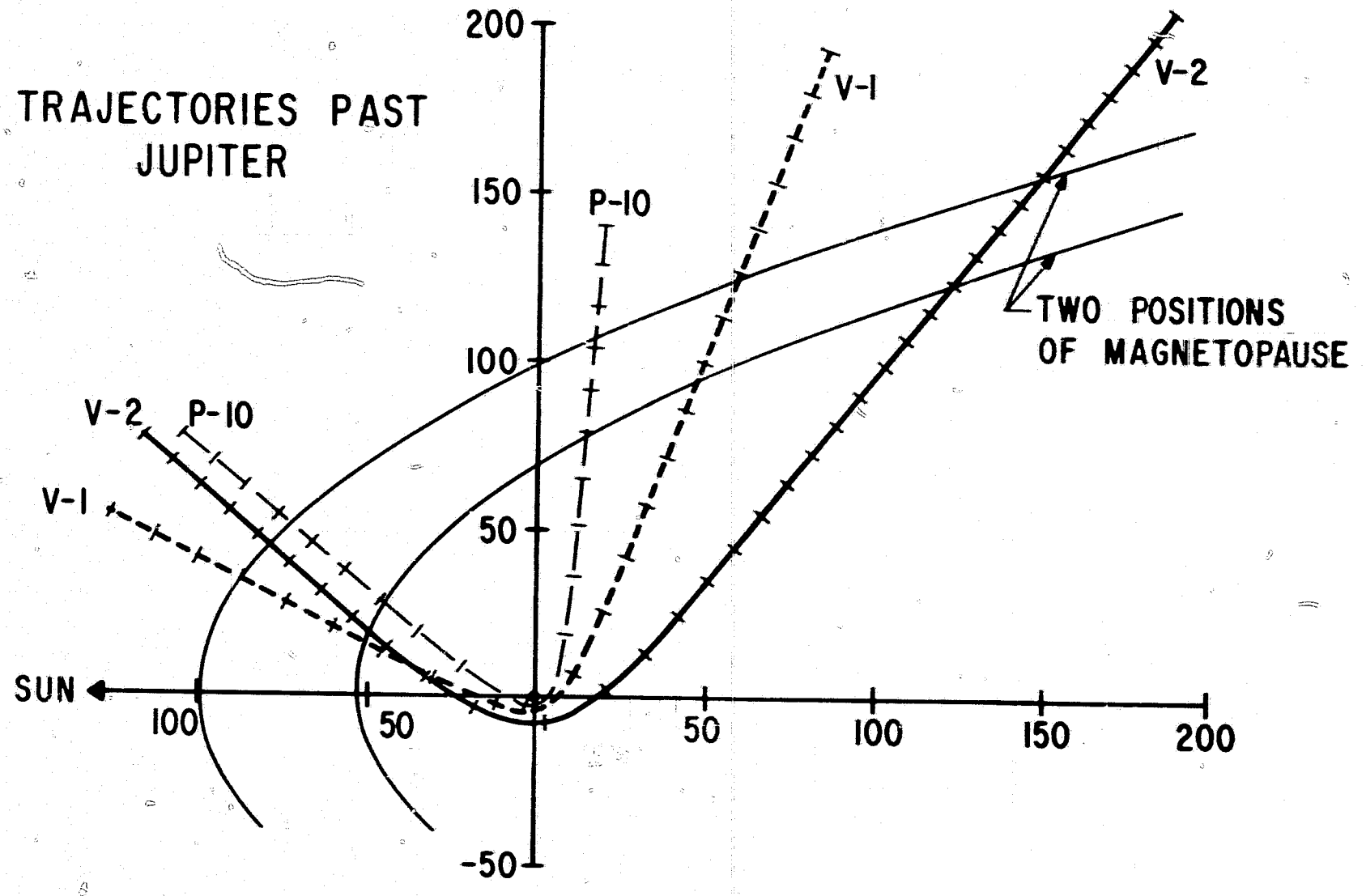
TRAJECTORIES PAST
JUPITER
200
150
100
50
-50
P-10
V-1
V-2
TWO POSITIONS
OF MAGNETOPAUSE
V-2
P-10
V-1
SUN
100
50
50
100
150
200

FIG. 1

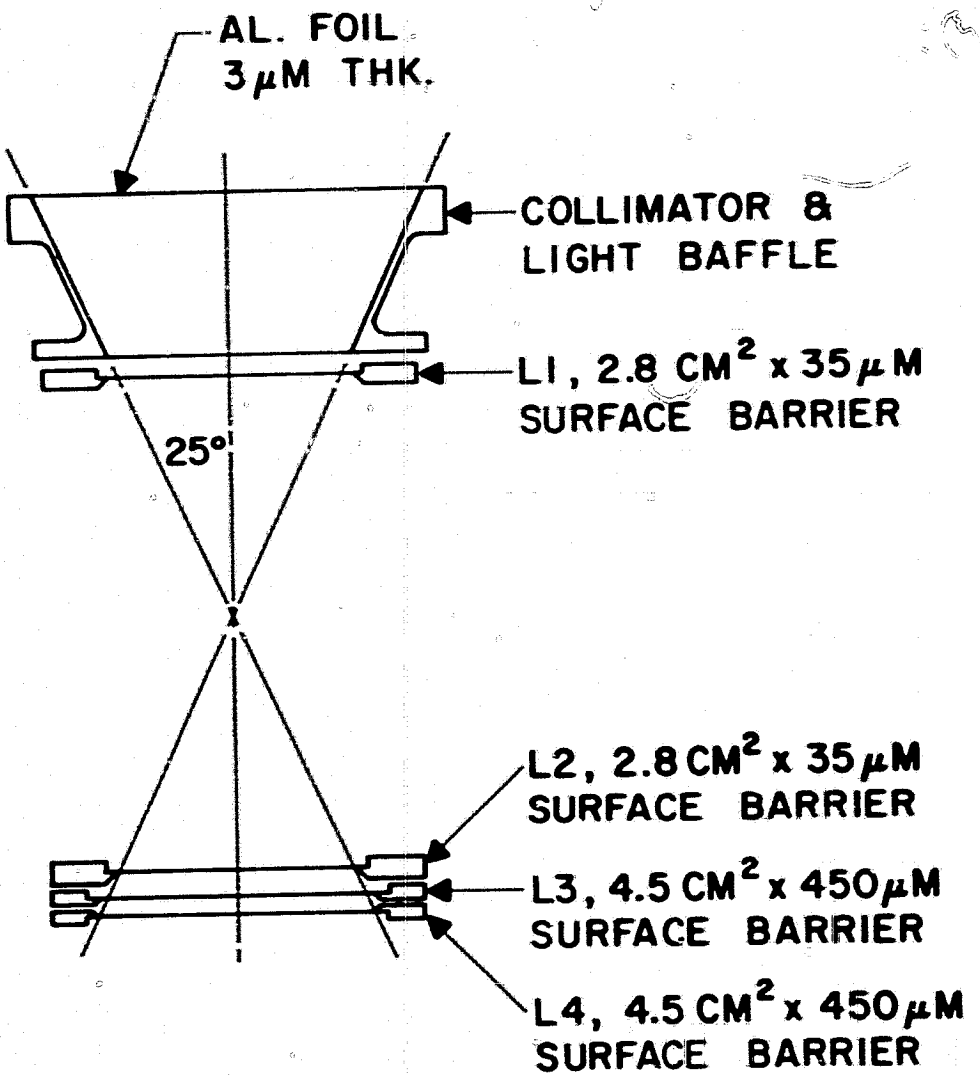

LOW ENERGY TELESCOPE (LET)

FIG. 2

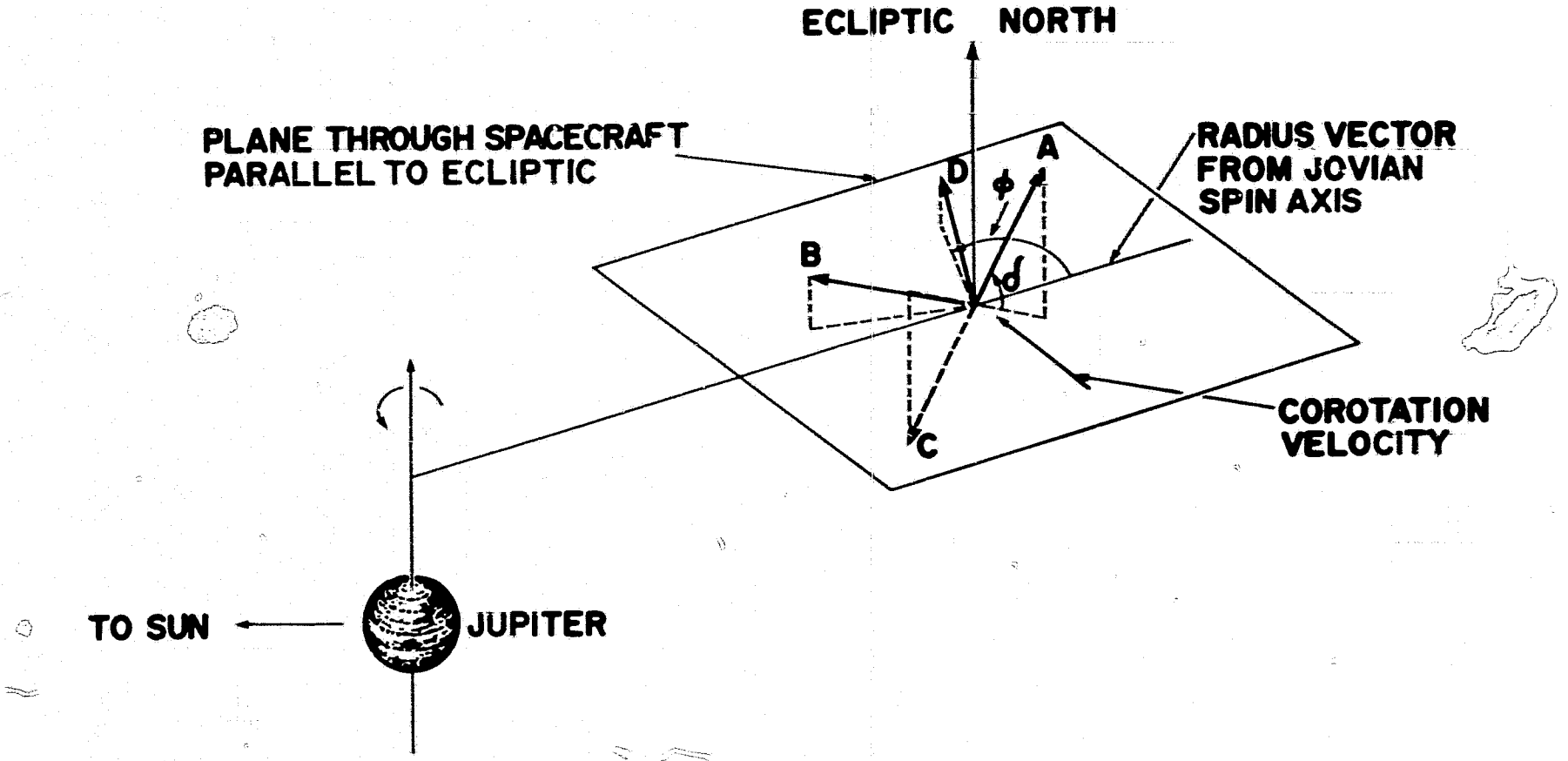
ECLIPTIC NORTH
PLANE THROUGH SPACECRAFT
PARALLEL TO ECLIPTIC
RADIUS VECTOR
FROM JOVIAN
SPIN AXIS
A
B
C
D
COROTATION
VELOCITY
TO SUN
JUPITER

FIG. 3

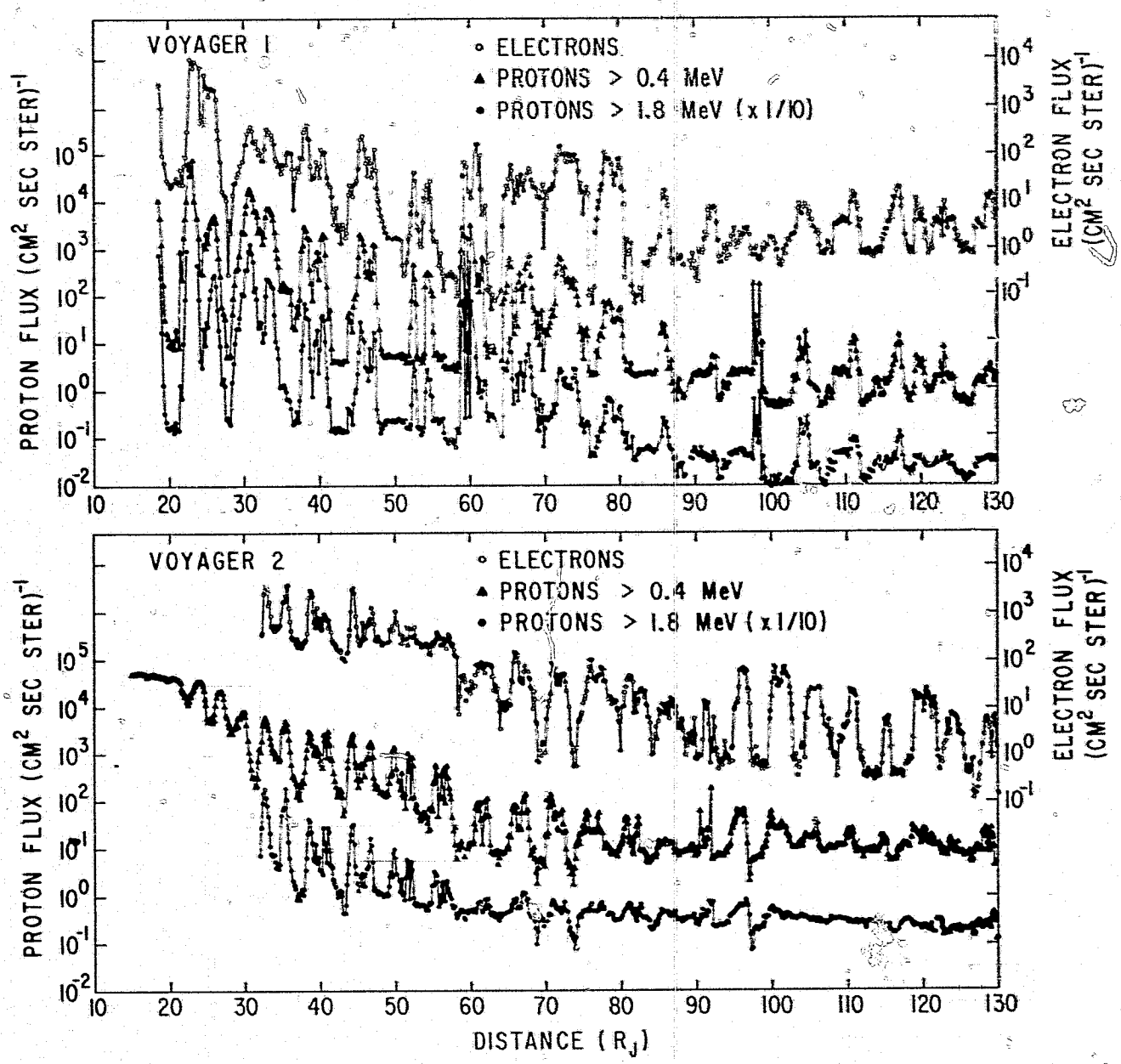

FIG. 4

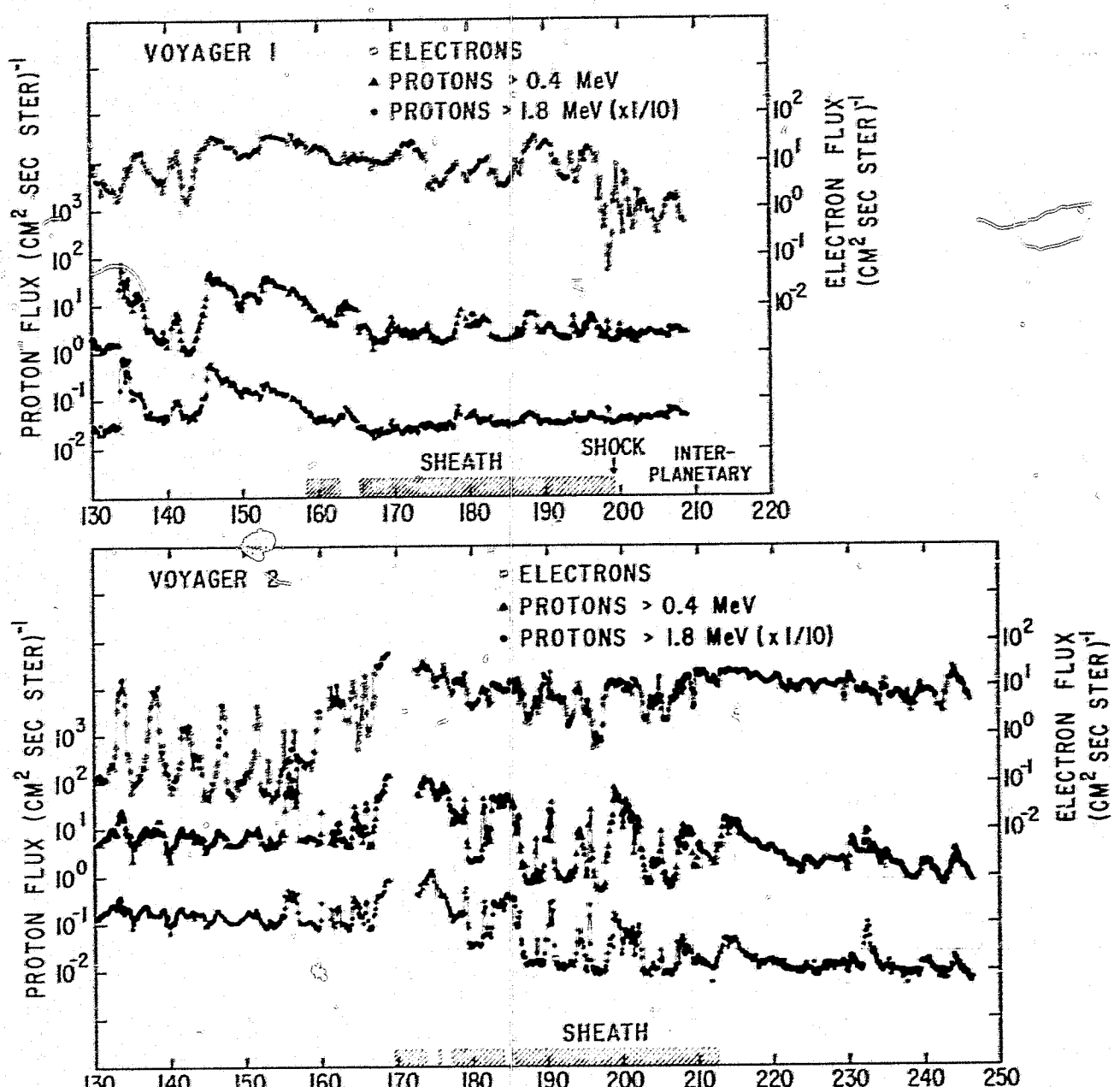
VOYAGER 1
ELECTRONS
PROTONS > 0.4 MeV
PROTONS > 1.8 MeV (x1/10)
PROTON FLUX (CM² SEC STER)⁻¹
ELECTRON FLUX (CM² SEC STER)⁻¹
SHEATH
SHOCK
INTER-PLANETARY
VOYAGER 2
ELECTRONS
PROTONS > 0.4 MeV
PROTONS > 1.8 MeV (x 1/10)
PROTON FLUX (CM² SEC STER)⁻¹
ELECTRON FLUX (CM² SEC STER)⁻¹
SHEATH
DISTANCE (R_J)

FIG. 5

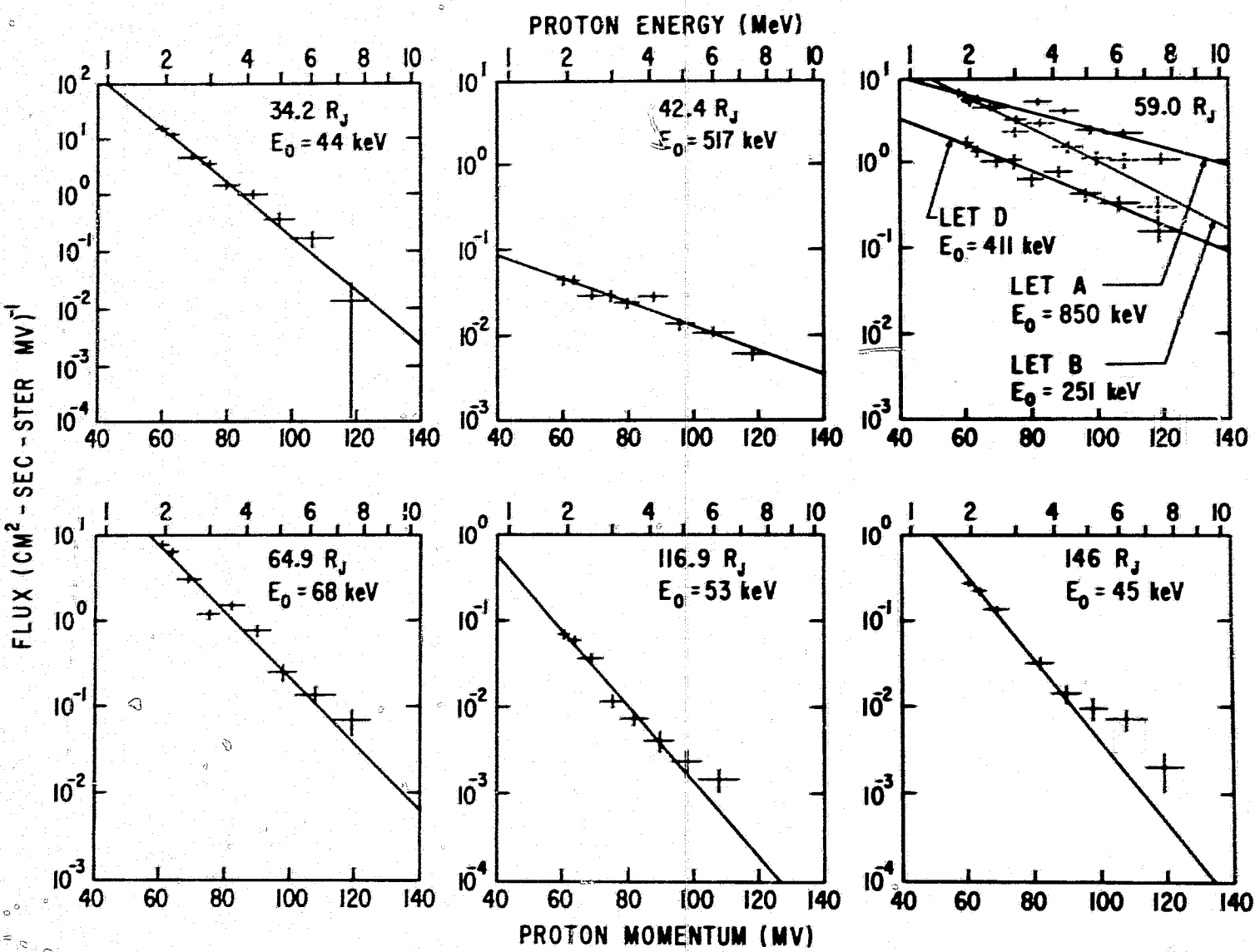
PROTON ENERGY (MeV)
FLUX (CM^2-SEC-STER MV)$^{-1}$
PROTON MOMENTUM (MV)
34.2 R_J
E_0 = 44 keV
42.4 R_J
E_0 = 517 keV
59.0 R_J
LET D
E_0 = 411 keV
LET A
E_0 = 850 keV
LET B
E_0 = 251 keV
64.9 R_J
E_0 = 68 keV
116.9 R_J
E_0 = 53 keV
146 R_J
E_0 = 45 keV

FIG. 6

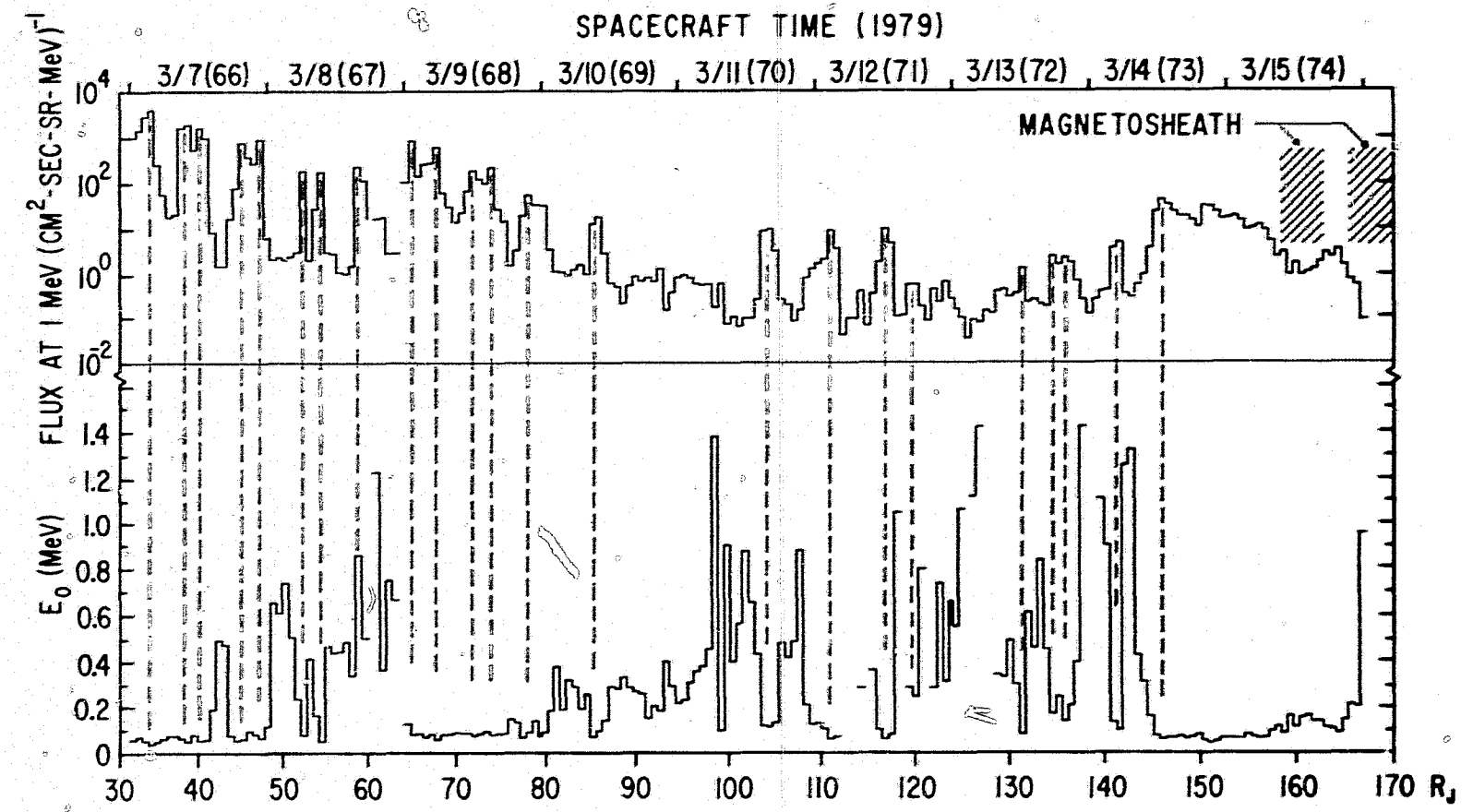
SPACECRAFT TIME (1979)
3/7(66)
3/8(67)
3/9(68)
3/10(69)
3/11(70)
3/12(71)
3/13(72)
3/14(73)
3/15(74)
MAGNETOSHEATH
FLUX AT 1 MeV (CM²-SEC-SR-MeV)⁻¹
10⁴
10²
10⁰
10⁻²
E₀ (MeV)
1.4
1.2
1.0
0.8
0.6
0.4
0.2
0
30
40
50
60
70
80
90
100
110
120
130
140
150
160
170 Rⱼ

FIG. 7

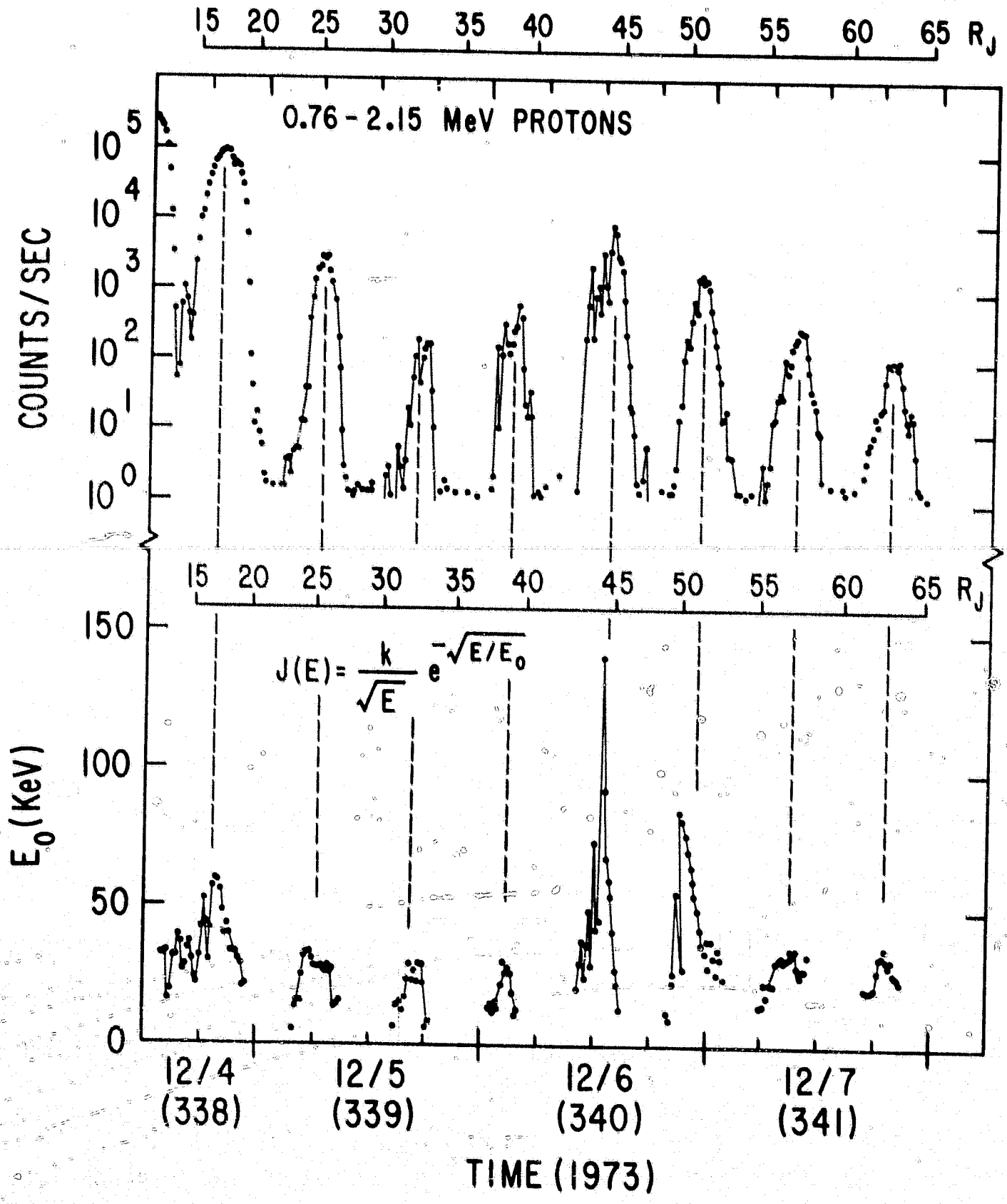

FIG. 8

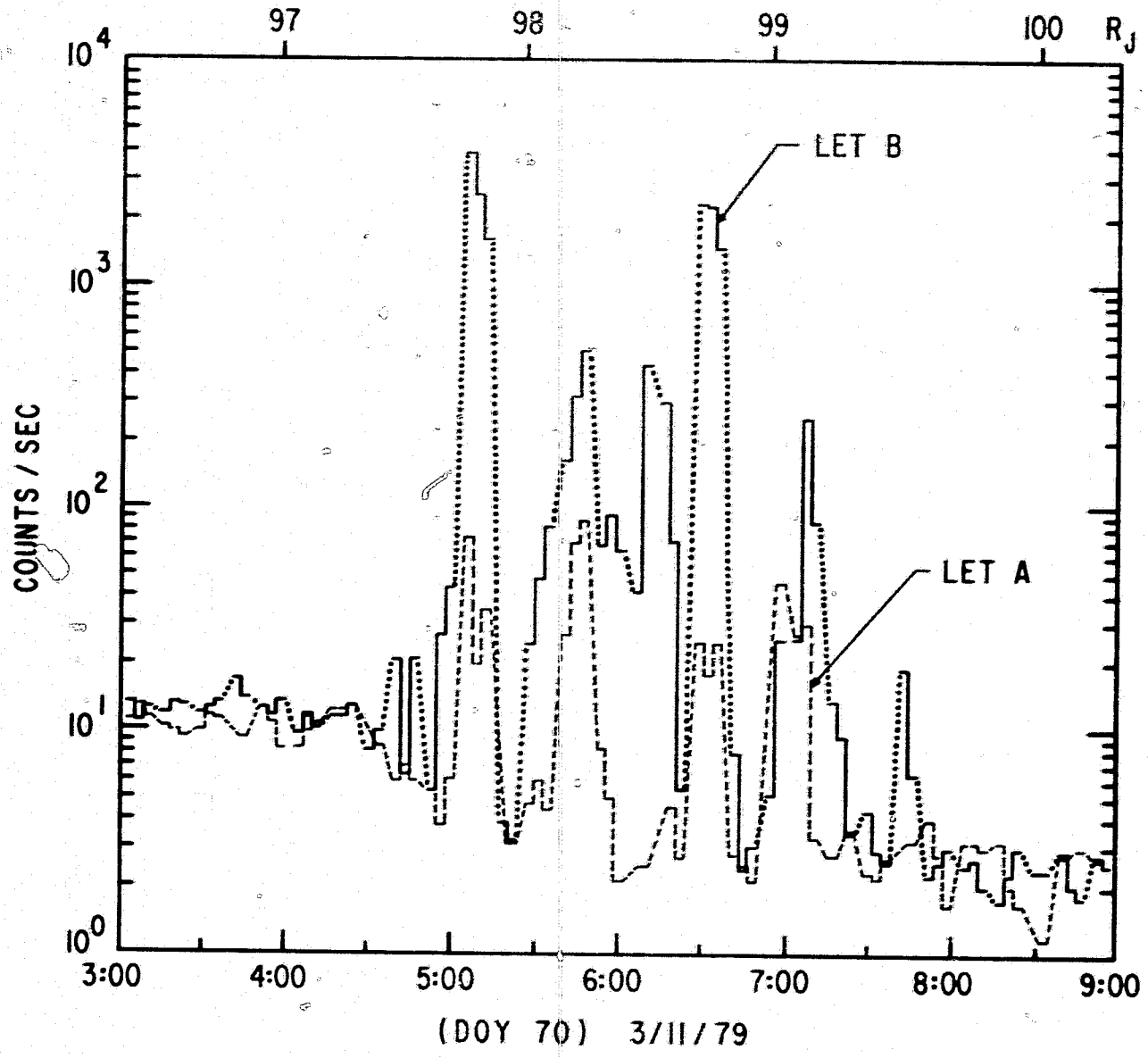
97
98
99
100
R_J
10^4
10^3
10^2
10^1
10^0
COUNTS / SEC
LET B
LET A
3:00
4:00
5:00
6:00
7:00
8:00
9:00
(DOY 70) 3/11/79

FIG. 9

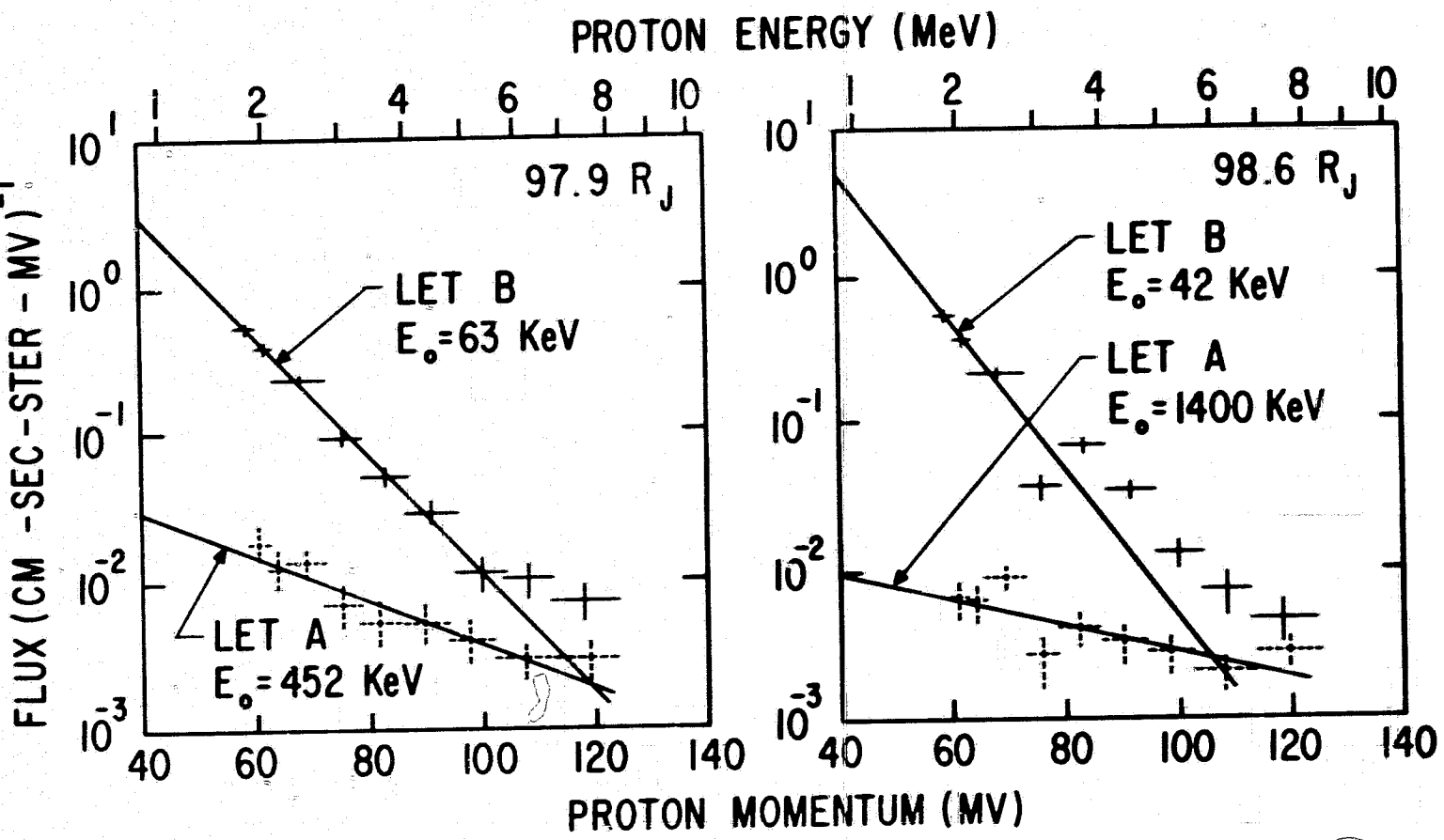
PROTON ENERGY (MeV)
1
2
4
6
8
10
97.9 R_J
LET B
E_o=63 KeV
LET A
E_o=452 KeV
98.6 R_J
LET B
E_o=42 KeV
LET A
E_o=1400 KeV
FLUX (CM -SEC-STER - MV)$^{-1}$
10^{1}
10^{0}
10^{-1}
10^{-2}
10^{-3}
40
60
80
100
120
140
PROTON MOMENTUM (MV)

FIG. 10

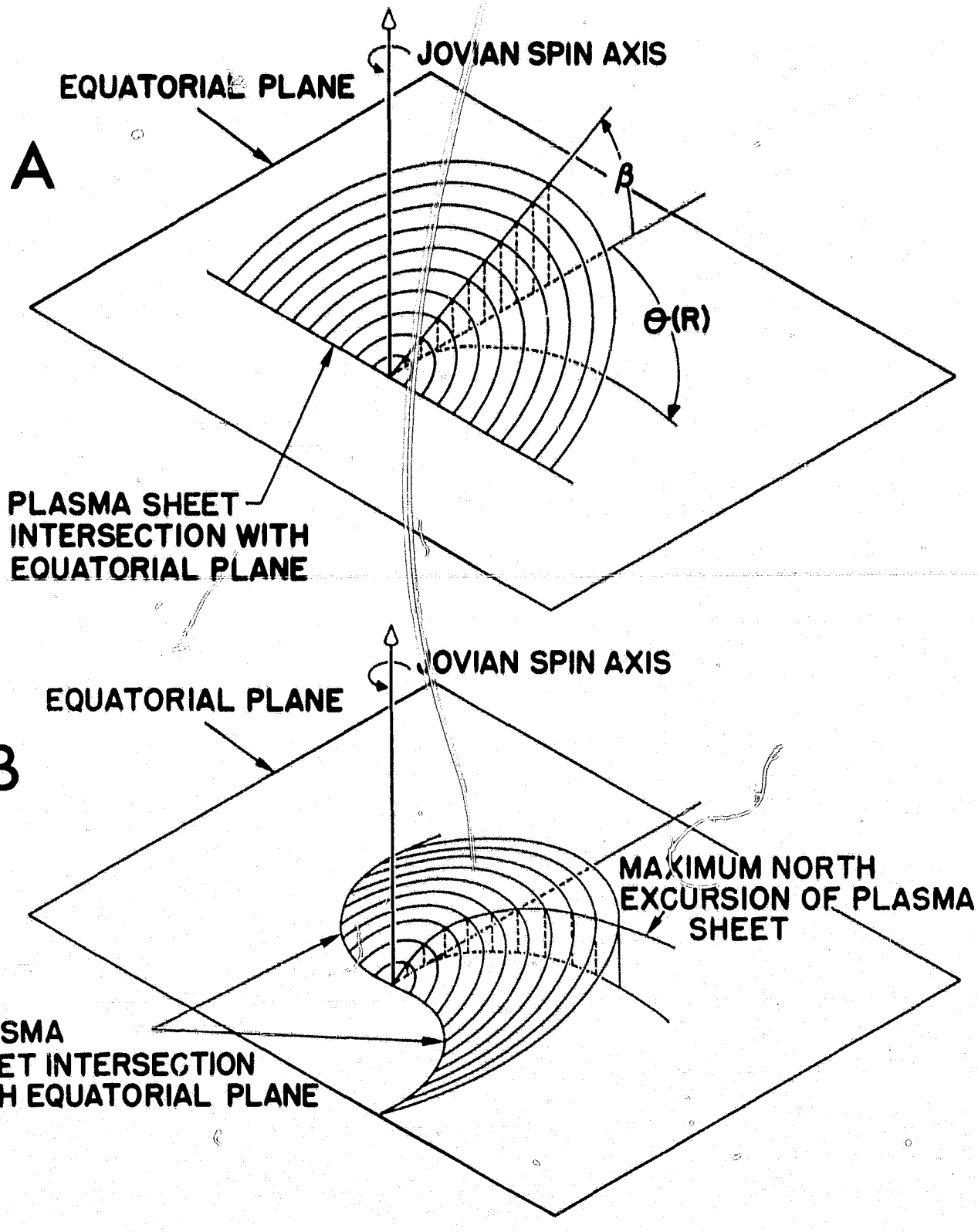
A
JOVIAN SPIN AXIS
EQUATORIAL PLANE
β
Θ(R)
PLASMA SHEET
INTERSECTION WITH
EQUATORIAL PLANE
B
JOVIAN SPIN AXIS
EQUATORIAL PLANE
MAXIMUM NORTH
EXCURSION OF PLASMA
SHEET
PLASMA
SHEET INTERSECTION
WITH EQUATORIAL PLANE

FIG. 11

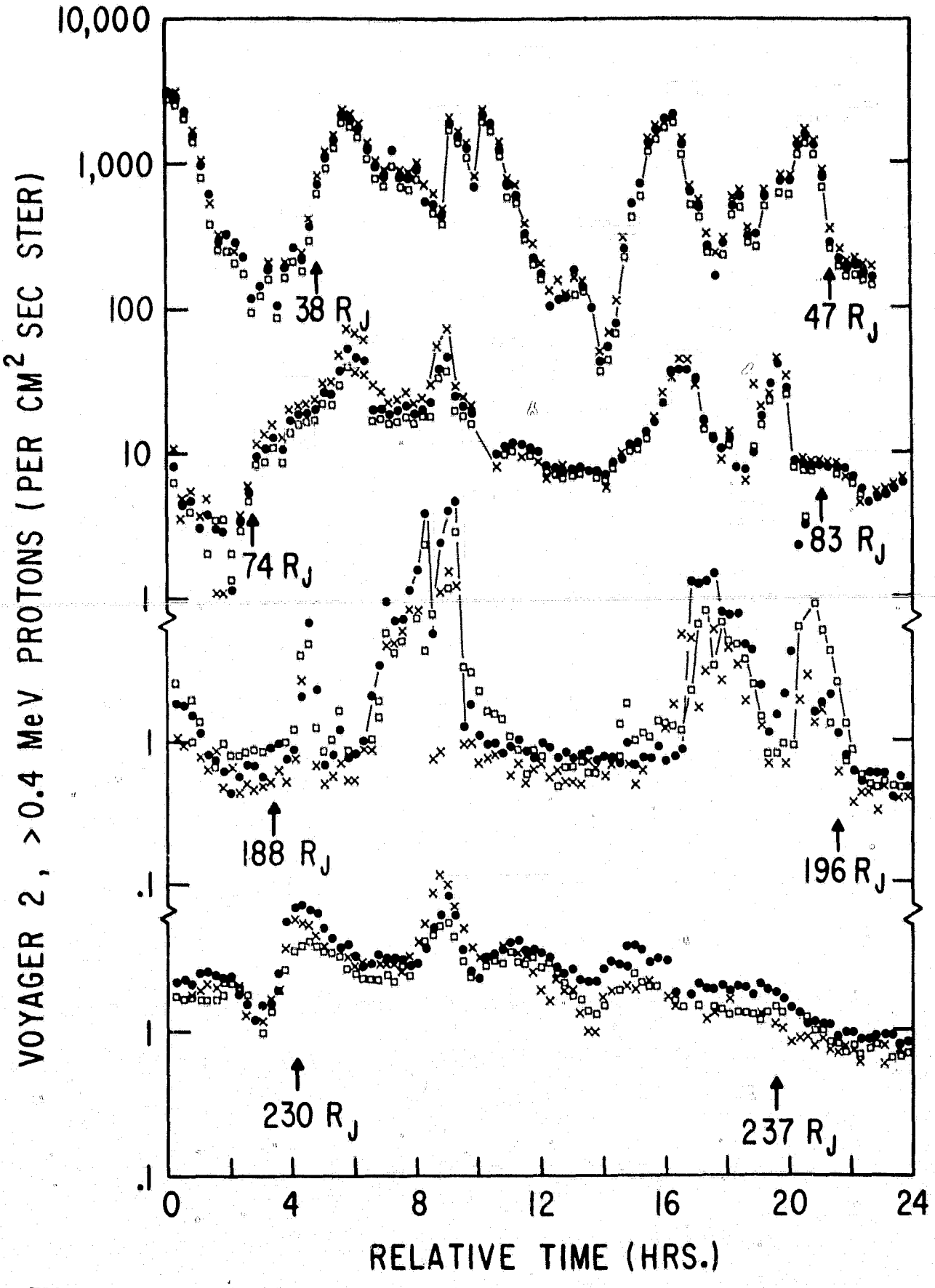
10,000
1,000
100
10
1
.1
VOYAGER 2, >0.4 MeV PROTONS (PER CM² SEC STER)
38 R_J
47 R_J
74 R_J
83 R_J
188 R_J
196 R_J
230 R_J
237 R_J
0
4
8
12
16
20
24
RELATIVE TIME (HRS.)

FIG. 12

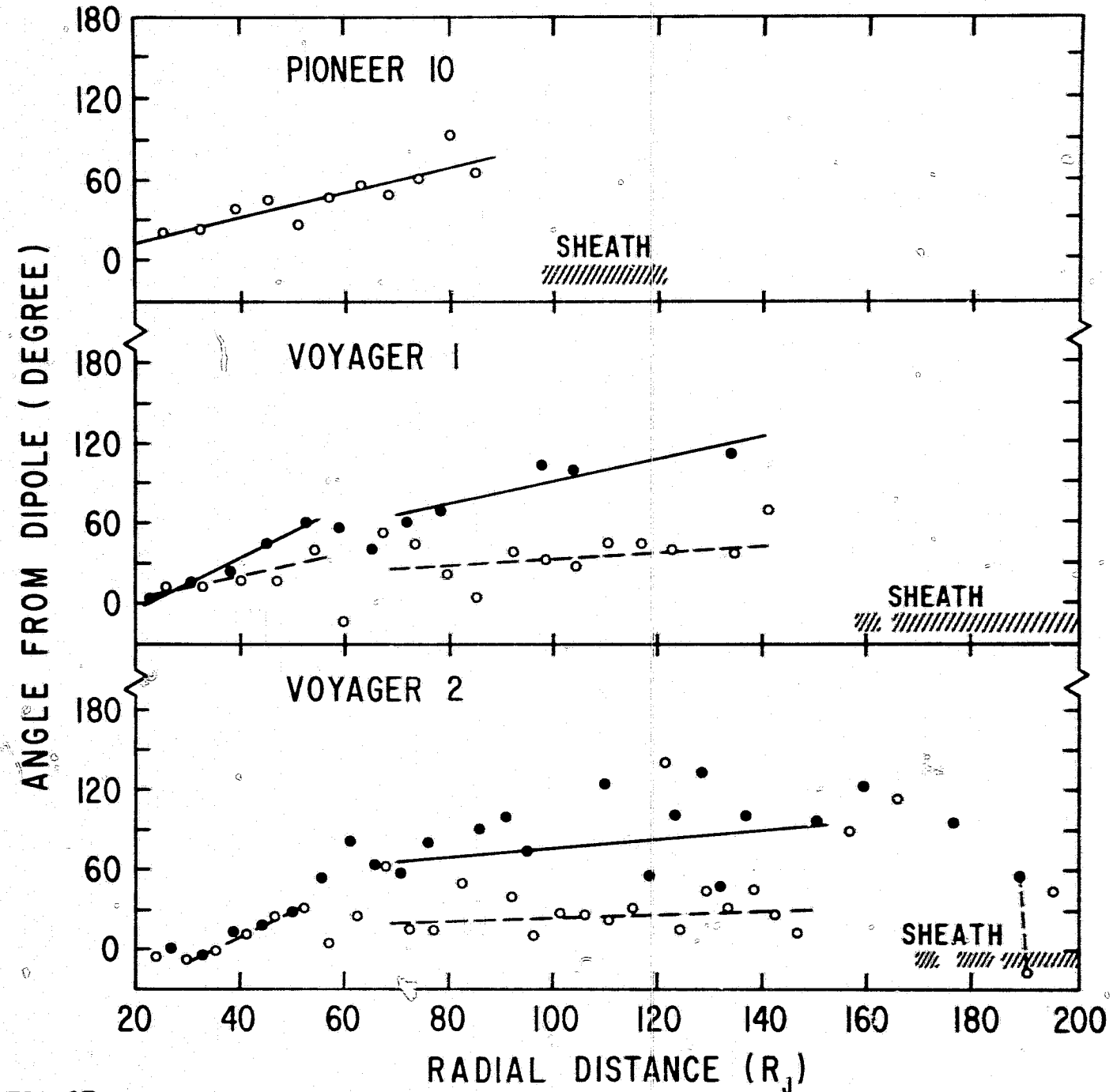
PIONEER 10
SHEATH
VOYAGER 1
SHEATH
VOYAGER 2
SHEATH
ANGLE FROM DIPOLE (DEGREE)
RADIAL DISTANCE (R_J)
0
60
120
180
20
40
60
80
100
120
140
160
180
200

FIG. 13

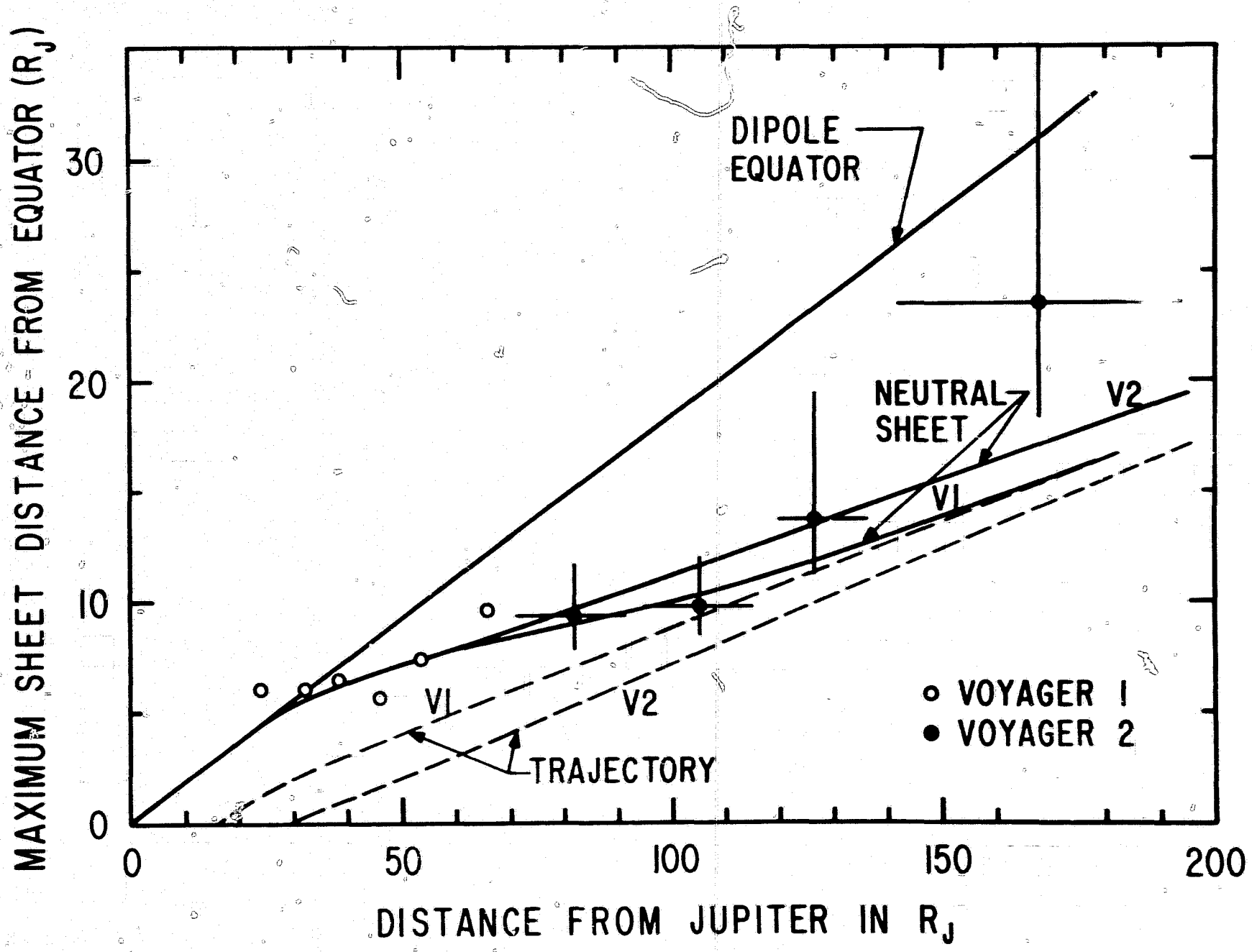
MAXIMUM SHEET DISTANCE FROM EQUATOR (R_J)
DISTANCE FROM JUPITER IN R_J
0
10
20
30
0
50
100
150
200
DIPOLE EQUATOR
NEUTRAL SHEET
V2
V1
V1
V2
TRAJECTORY
VOYAGER 1
VOYAGER 2

FIG. 14

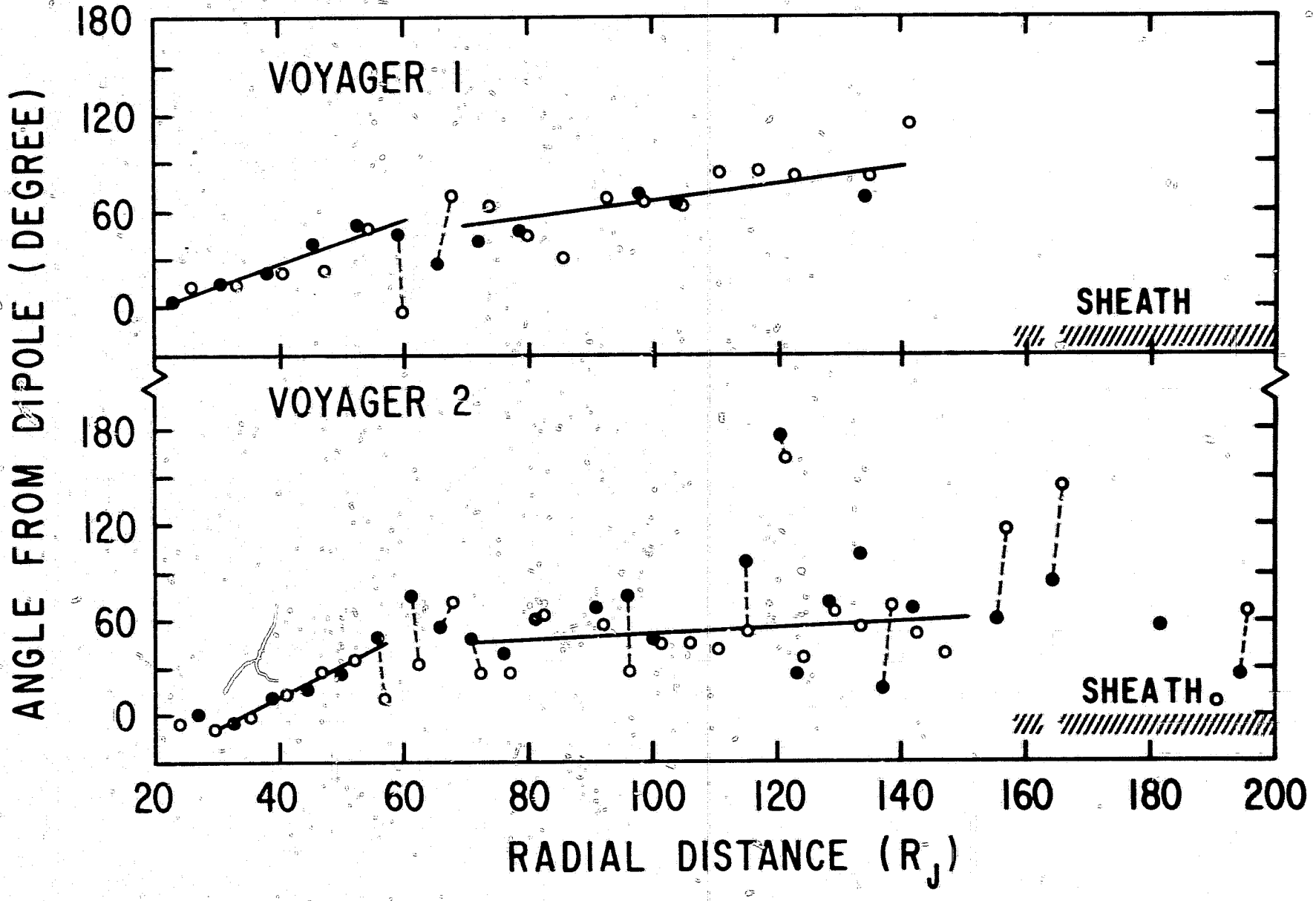
VOYAGER 1
VOYAGER 2
SHEATH
SHEATH
ANGLE FROM DIPOLE (DEGREE)
RADIAL DISTANCE (R_J)
0
60
120
180
20
40
60
80
100
120
140
160
180
200

FIG. 15

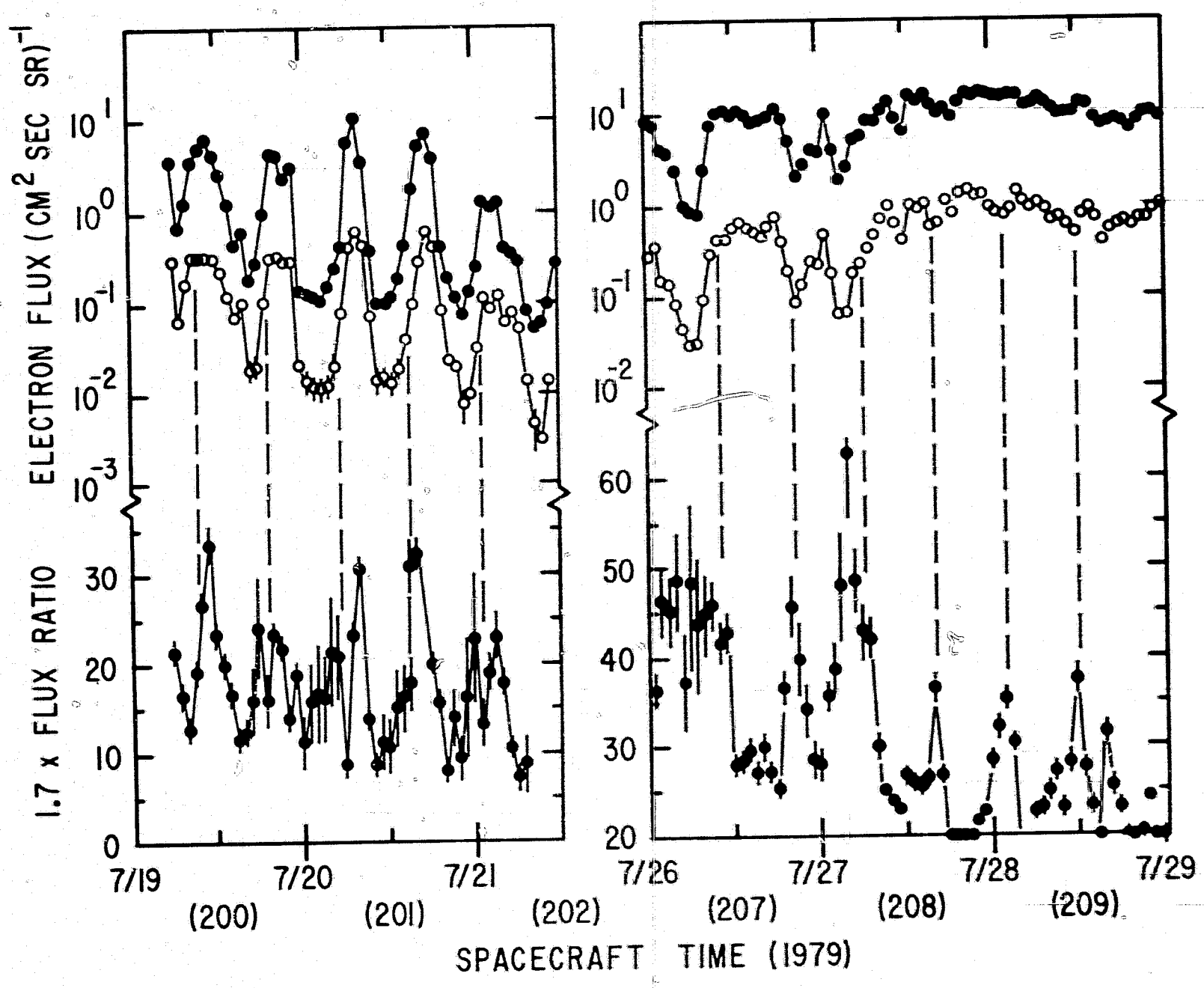
ELECTRON FLUX (CM^2 SEC SR)$^{-1}$
1.7 x FLUX RATIO
10^1
10^0
10^{-1}
10^{-2}
10^{-3}
0
10
20
30
20
30
40
50
60
7/19
7/20
7/21
7/26
7/27
7/28
7/29
(200)
(201)
(202)
(207)
(208)
(209)
SPACECRAFT TIME (1979)

FIG. 16

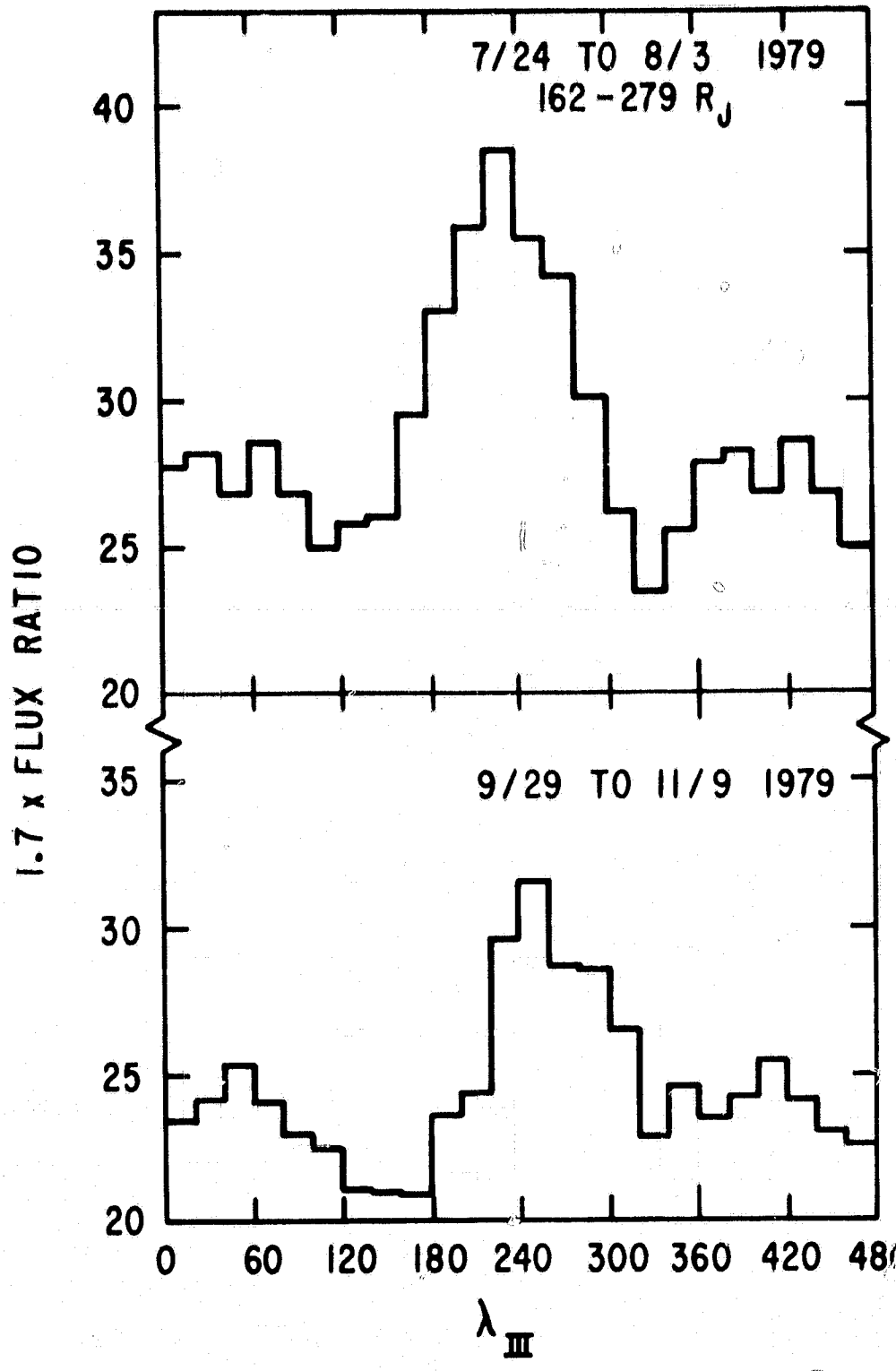
7/24 TO 8/3 1979
162 - 279 R_J
9/29 TO 11/9 1979
1.7 x FLUX RATIO
40
35
30
25
20
35
30
25
20
0
60
120
180
240
300
360
420
480
λ_{III}

FIG. 17

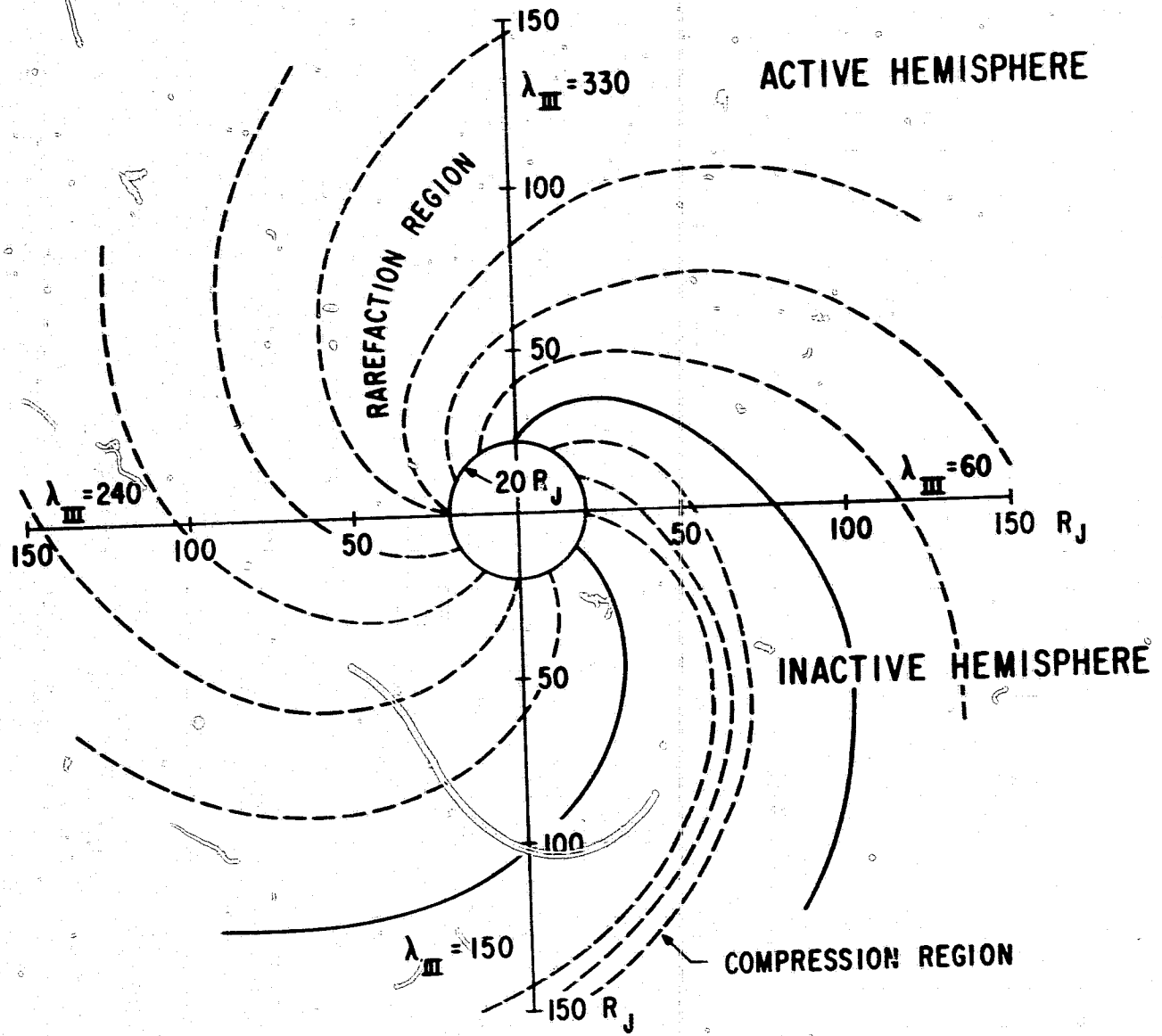
150
λ_{III}=330
ACTIVE HEMISPHERE
RAREFACTION REGION
100
50
λ_{III}=60
20 R_J
λ_{III}=240
150
100
50
50
100
150 R_J
INACTIVE HEMISPHERE
50
100
λ_{III}=150
COMPRESSION REGION
150 R_J

FIG. 18

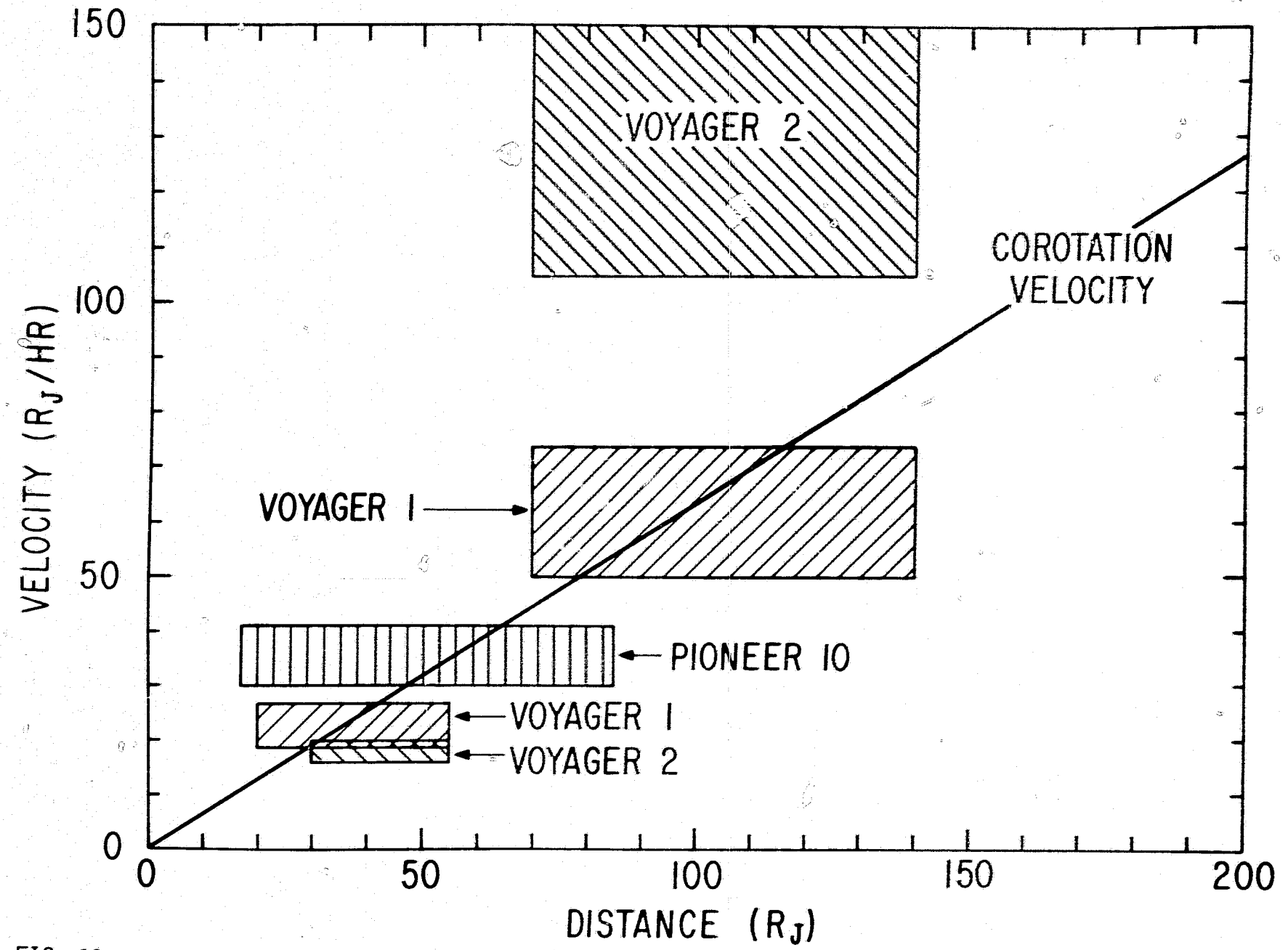
150
100
50
0
VELOCITY (R_J/HR)
VOYAGER 2
COROTATION
VELOCITY
VOYAGER 1
PIONEER 10
VOYAGER 1
VOYAGER 2
0
50
100
150
200
DISTANCE (R_J)

FIG. 19